MARTIN MARIETTA ENERGY SYSTEMS LIBRARIES

3 4456 0369379 6

ornl

ORNL/TM-12212

OAK RIDGE
NATIONAL
LABORATORY

MARTIN MARIETTA

High-Temperature Corrosion of Ceramic-Ceramic Composites in a Waste Incinerator Environment

J. R. Keiser
J. I. Federer
T. J. Henson
D. L. Hindman

OAK RIDGE NATIONAL LABORATORY
CENTRAL RESEARCH LIBRARY
CIRCULATION SECTION
4500N ROOM 175
LIBRARY LOAN COPY
DO NOT TRANSFER TO ANOTHER PERSON
If you wish someone else to see this report, send in name with report and the library will arrange a loan.
UCN-7969 (3 9-77)

MANAGED BY
MARTIN MARIETTA ENERGY SYSTEMS, INC.
FOR THE UNITED STATES
DEPARTMENT OF ENERGY

This report has been reproduced directly from the best available copy.

Available to DOE and DOE contractors from the Office of Scientific and Technical Information, P.O. Box 62, Oak Ridge, TN 37831; prices available from (615) 576-8401, FTS 626-8401.

Available to the public from the National Technical Information Service, U.S. Department of Commerce, 5285 Port Royal Rd., Springfield, VA 22161.

This report was prepared as an account of work sponsored by an agency of the United States Government. Neither the United States Government nor any agency thereof, nor any of their employees, makes any warranty, express or implied, or assumes any legal liability or responsibility for the accuracy, completeness, or usefulness of any information, apparatus, product, or process disclosed, or represents that its use would not infringe privately owned rights. Reference herein to any specific commercial product, process, or service by trade name, trademark, manufacturer, or otherwise, does not necessarily constitute or imply its endorsement, recommendation, or favoring by the United States Government or any agency thereof. The views and opinions of authors expressed herein do not necessarily state or reflect those of the United States Government or any agency thereof.

ORNL/TM-12212

310 95F

Metals and Ceramics Division

HIGH-TEMPERATURE CORROSION OF CERAMIC-CERAMIC COMPOSITES IN A WASTE INCINERATOR ENVIRONMENT

J. R. Keiser
J. I. Federer
T. J. Henson
D. L. Hindman

Date Published: January 1993

NOTICE: This document contains information of a preliminary nature. It is subject to revision or correction and therefore does not represent a final report.

Prepared for the
U.S. Department of Energy
Assistant Secretary for Conservation and Renewable Energy
Office of Industrial Technologies
ED 40 02 00 0

Prepared by the
OAK RIDGE NATIONAL LABORATORY
Oak Ridge, Tennessee 37831-6285
managed by
MARTIN MARIETTA ENERGY SYSTEMS, INC.
for the
U.S. DEPARTMENT OF ENERGY
under contract DE-AC05-84OR21400

MARTIN MARIETTA ENERGY SYSTEMS LIBRARIES

3 4456 0369379 6

TABLE OF CONTENTS

	Page
LIST OF FIGURES	v
LIST OF TABLES	vii
ABSTRACT	1
1. INTRODUCTION	1
2. MATERIALS	4
3. EXPOSURE CONDITIONS	6
4. RESULTS	8
4.1 VISUAL EXAMINATION	8
4.2 MICROSTRUCTURAL EXAMINATION	11
4.3 ELECTRON MICROPROBE EXAMINATION	15
4.3.1 Continuous-Filament Composite with an Alumina Matrix, 166A(x)	15
4.3.2 Continuous-Filament Ceramic Composite with an Alumina Matrix, Zirconia Coating Initially Applied, 166A/Z(x)	24
4.3.3 Continuous-Filament Ceramic Composite with a Partially Stabilized Zirconia Matrix, 166Z(x)	29
4.3.4 Alumina Matrix Composite Strengthened with Silicon Carbide Particles, AS(x)	38
5. DISCUSSION AND CONCLUSIONS	44
6. ACKNOWLEDGMENTS	47
7. REFERENCES	47

LIST OF FIGURES

Figure		Page
1	Before-test sections of as-fabricated ceramic composite tubes that formed a corrosion probe in the waste incinerator. Composite identification, left to right: 166A/Z, 166Z, AS, and 166A	7
2	A corrosion probe following an exposure of 6 months in the waste incinerator. Discoloration and deposits are apparent. Composite identification, left to right: 166Z(6), 166A(6), AS(6), and 166A/Z(6)	9
3	The zirconia matrix composite, 166Z(6), following an exposure of 6 months in the waste incinerator. The alloy 718 plate, which was pinned to an alloy 600 tube, retained the tube sections during exposure in the incinerator	10
4	Light micrographs of PRD 166/alumina composite [166A(6)] after 6 months' exposure in a hazardous waste incinerator	12
5	Light micrograph of PRD 166/alumina composite with a zirconia surface coating [166A/Z(4)] after 4 months' exposure in a hazardous waste incinerator	13
6	Light micrograph of PRD 166/zirconia composite [166Z(6)] after 6 months' exposure in a hazardous waste incinerator	14
7	Light micrographs of silicon carbide-particulate-strengthened alumina [AS(6)] after 6 months' exposure in a hazardous waste incinerator	16
8	Back-scattered electron and characteristic X-ray images of the unexposed continuous-filament composite with an alumina matrix [166A(0)]	17
9	Back-scattered electron and characteristic X-ray images of the continuous-filament composite with an alumina matrix after a 3-month exposure [166A(3)]	18
10	Back-scattered electron and characteristic X-ray images of the continuous-filament composite with an alumina matrix after a 4-month exposure [166A(4)]	20
11	Back-scattered electron and characteristic X-ray images of the continuous-filament composite with an alumina matrix after a 6-month exposure [166A(6)]	21
12	Light micrographs of composite 166A(6) showing locations where electron microprobe semiquantitative elemental measurements were made	23

Figure		Page
13	Back-scattered electron and characteristic X-ray images of the unexposed continuous-filament composite with an alumina matrix and zirconia surface coating [166A/Z(0)]	25
14	Back-scattered electron and characteristic X-ray images of the continuous-filament composite with an alumina matrix and zirconia surface coating after an exposure of 4 months [166A/Z(4)]	26
15	Back-scattered electron and characteristic X-ray images of the continuous-filament composite with an alumina matrix and zirconia surface coating after an exposure of 6 months [166A/Z(6)]	28
16	Back-scattered electron and characteristic X-ray images of the unexposed continuous-filament composite with a zirconia matrix [166Z(0)]	30
17	Back-scattered electron and characteristic X-ray images of the continuous-filament composite with a zirconia matrix after an exposure of 3 months [166Z(3)]	31
18	Back-scattered electron and characteristic X-ray images of the continuous-filament composite with a zirconia matrix after an exposure of 4 months [166Z(4)]	33
19	Back-scattered electron and characteristic X-ray images of the continuous-filament composite with a zirconia matrix after an exposure of 6 months [166Z(6)]	34
20	Back-scattered electron and characteristic X-ray images of sample 166Z(6) showing locations where electron microprobe semiquantitative elemental measurements were made	36
21	Back-scattered electron and characteristic X-ray images of the silicon carbide-particulate-strengthened alumina composite after an exposure of 3 months [AS(3)]	40
22	Back-scattered electron and characteristic X-ray images of the silicon carbide-particulate-strengthened alumina composite after an exposure of 6 months [AS(6)]	42

LIST OF TABLES

Table		Page
1	Designation and constituents of materials exposed to flue gases in a waste incinerator at a maximum temperature of 900°C	7
2	Concentration at various sites within composite 166A(6)	22
3	Analysis of various regions at or near the surface of composite 166Z(6)	39

HIGH-TEMPERATURE CORROSION OF CERAMIC-CERAMIC COMPOSITES IN A WASTE INCINERATOR ENVIRONMENT*

J. R. Keiser, J. I. Federer, T. J. Henson, and D. L. Hindman†

ABSTRACT

Three types of ceramic composite were exposed to the flue gases of a hazardous waste incinerator to assess their corrosion behavior. One composite consisted of continuously wound filaments of Al_2O_3-23 wt % ZrO_2 in an alumina matrix. This composite was tested, both uncoated and coated, with zirconia on the outer surface. The second composite type consisted of the same fiber but in a zirconia matrix. The third composite consisted of an alumina matrix strengthened with silicon carbide particles. Tubes of these materials were exposed in the waste incinerator at about 900°C for times up to six months. Two principal results of exposure were revealed by optical microscopy and electron microprobe examinations: flue gas constituents either penetrated the uncoated alumina matrix of the filament-wound composite, apparently through porosity in the matrix, or deposited on the surfaces of the other composite types where reaction and bonding occurred. Neither event caused significant microstructural degradation of the composites, although the extent of reaction in the composite with a zirconia matrix suggests that degradation could be a problem under more severe conditions. Apparently, the concentration of penetrating species was too small to form a significant amount of new compounds that could cause degradation within the alumina matrix of the filament-wound composite, and the temperature was too low for the deposits on the surface of the other two types of composites to react significantly with the materials during the longest exposure of 6 months. The zirconia coating on the alumina matrix composite was not adherent enough to permit an assessment of its effect.

---

1. INTRODUCTION

One activity of the U.S. Department of Energy (DOE) is support of research and development programs directed toward more efficient use of the nation's energy resources.

---

*Research sponsored by the U.S. Department of Energy, Assistant Secretary for Conservation and Renewable Energy, Office of Industrial Technologies, Industrial Energy Efficiency Division, under contract DE-AC05-84OR21400 with Martin Marietta Energy Systems, Inc.

†Babcock & Wilcox Company, Lynchburg, Va.

Numerous studies and surveys have revealed that much sensible heat is lost or wasted from many industrial processes in the form of high-temperature flue gases. Therefore, a significant part of the DOE effort has focused on innovative energy recovery methods as well as more efficient use of energy in industrial processes.[1,2] A current program involves a waste heat recuperator that is being developed by Babcock & Wilcox (B&W) Company under a cost-sharing contract with DOE.[3,4] This type of recuperator is intended to recover heat from "dirty" flue gases (for example, those derived from combustion of municipal or hazardous wastes). High-temperature corrosion of materials is a serious concern in these facilities, so testing and evaluation of materials of construction is an important part of the recuperator development process.

Recuperator tubes will be exposed to high-temperature incinerator flue gases so that heat can be transferred from the flue gases to air inside the tubes. The heated air can be used for a variety of purposes (for example, preheating of raw materials, combustion air for gas or oil burners, or to drive a gas turbine to produce electrical power). These applications require the air to be heated to a high temperature to attain the desired efficiency; therefore, the tubes will be exposed to flue gases at 1000 to 1100°C, and the air will be heated to about 900°C. Most structural alloys used in heat exchangers and other high-temperature applications, such as iron- and nickel-based alloys, do not have adequate strength and corrosion resistance at these temperatures. Special high-temperature alloys might be considered, but even these alloys have limited strength at these temperatures and would be susceptible to serious damage during high-temperature excursions. For this reason, B&W intends to use recuperator tubes fabricated of ceramic materials.

The tubes will be subjected to stresses from several sources, such as those imposed on the tubes by their own weight and those caused by the force of impinging particulates and flue gases. Pressurization of the heated air within the tubes normally will be too small to produce significant hoop and axial stresses, but this possibility should be recognized as a potential

source of stress in the event of a pressure control problem. The most significant stresses, and probably the most difficult to quantify, will be those caused by thermal gradients through the tube wall, along the length, and around the circumference. All of these sources acting together produce a complicated stress state that could exceed the fracture strength of the material under severe conditions.

Certain structural ceramic materials, for example, those based on alumina (Al_2O_3) and zirconia (ZrO_2), have the inherent strength required for recuperator tubes; that is, samples of these materials with properly prepared surfaces have high average strengths and exhibit only small deviations from the average values. However, as-fabricated monolithic forms of these materials having no special surface preparation exhibit much lower average strengths and much larger deviations. Strengths of as-fabricated monolithic forms are directly related to surface flaws that serve as crack initiators under stress, but machining the tubes to produce surfaces with fewer flaws would be prohibitively expensive. Moreover, corrosion caused by exposure to high-temperature flue gases can cause new flaws in either as-fabricated or machined surfaces, so a flawed surface is a probable condition during extended service.

Other disadvantages of monolithic materials are a lack of toughness and resistance to thermal shock. Low toughness can result in brittle failure without significant deformation. Sensitivity to thermal shock means that cracks can form during rapid heating or cooling, or possibly because of the thermal gradient across the wall of the tube during normal operation. All of these strength-limiting characteristics are undesirable in such critical components as recuperator tubes because of the economic penalty associated with system downtime. Because of these possible problems with strength, toughness, resistance to thermal shock, and high-temperature corrosion, monolithic materials are not considered to be candidates for recuperator tubes for the B&W application. To overcome these problems, B&W has developed oxide ceramic composites with much higher toughness, better resistance to thermal shock, and

adequate strength in the as-fabricated condition. In addition, B&W is evaluating a commercially available composite material consisting of an alumina matrix strengthened with SiC particles.*

To evaluate whether high-temperature corrosion would seriously affect the integrity of these ceramic recuperator tubes, B&W exposed tubes of both the filament-toughened composites and the SiC particle-strengthened composite to the high-temperature flue gases of an industrial waste incinerator owned and operated by E. I. DuPont in Wilmington, Delaware. Oak Ridge National Laboratory (ORNL) assisted B&W in this effort by examining exposed samples to characterize the microstructures and corrosion products. This information, along with room- and elevated-temperature mechanical property data determined by B&W, will be used to select a material for recuperator tubes. This report presents the results of microscopic examination of as-fabricated and exposed samples.

2. MATERIALS

The ceramic composites developed by B&W were strengthened and toughened with 20-μm-diam continuous filaments of PRD-166**, a fiber composed of Al_2O_3-23 wt % ZrO_2 (Al_2O_3-20 mole % ZrO_2). The filaments were fabricated into tubular forms with both alumina- and zirconia-based matrices by a proprietary process. Properties of the finished tubes were influenced by the matrix composition (for example, additives to promote sintering), relative proportions of matrix and filament, winding pattern of the filament, and sintering conditions for consolidation. Although the process is proprietary, the general fabrication method involved first winding the filaments onto a mandrel in a hoop/helical

---

*DuPont-Lanxide Corporation.

**DuPont Corporation, Wilmington, Del.

winding pattern to create a tubular preform. Hoop winding refers to winding around a tubular mandrel without significant advance (angle of advance ≈ 0 degrees) along the long axis of the mandrel between adjacent turns (similar to thread on a spool). In helical winding, the angle of advance is >> 0 degrees, e.g., 45 degrees, so that there is significant interlocking of overlapping layers of wound filament. Hoop-wound forms are stronger radially than axially, whereas helical winding imparts axial strength to the form. The filament-wound preform was then impregnated with the matrix material, and the resulting "green" composite was sintered to densify the matrix.

B&W fabricated filament-wound tubes with both alumina- and zirconia-based matrices. In composites with an alumina matrix, the filaments were coated with zirconia to minimize reaction (sintering) between the filament and matrix. As will be shown, the coating on the filaments generally was not very adherent. Because the alumina matrices contained about 35% porosity in the as-fabricated condition, some tubes with an alumina matrix were coated with zirconia to minimize penetration of flue gas constituents into the matrix. Composites with a zirconia matrix had about 25% porosity, and the zirconia was partially stabilized with yttria. No coating was applied to tubes with a zirconia matrix because earlier results had indicated that flue gas constituents did not significantly penetrate the material. The tubes had a diameter of about 100 mm, a wall thickness of about 3.5 mm, and the filaments constituted about 50 vol % of the composites.

The alumina matrix material strengthened with SiC particles was also fabricated into tubes by a proprietary process involving starting materials, processing temperatures, additives to promote consolidation, and coatings. This material consisted of ≈50 vol % SiC particles (maximum size ≈25 μm) in an alumina matrix. A small amount of aluminum (a few percent) in the microstructure was residue from the fabrication process. The tubes had a diameter of

≈121 mm and a wall thickness of 6.4 mm. The constituents of the composites are summarized in Table 1. The designation of the composites shown in Table 1 will be used in this report.

Sections of as-fabricated tubes with both types of matrix materials were used to form corrosion probes as shown in Fig. 1. A corrosion probe was prepared by mounting the tube sections on a smaller diameter Inconel alloy 600 tube, which was pinned to an alloy 718 plate on one end (the left end in Fig. 1) to retain the ceramic tubes on the metal tube. Sintered zirconia fiber plugs separated the materials as shown in Fig. 1 and limited penetration of flue gases into the interior of the tube sections. Samples from tubes, such as these, were also used for determination of as-fabricated mechanical properties (by B&W), and sections of such tubes were used for pre-exposure microstructural characterization (by ORNL).

Thus, three types of ceramic composite tubes were exposed to flue gases in a waste incinerator: PRD166 filament-strengthened alumina with and without a zirconia coating on the outer surface [166A(x) and 166A/Z(x)], respectively; PRD166 filament-strengthened zirconia [166Z(x)]; and alumina strengthened with silicon carbide particles [AS(x)]. After the exposure, samples of each type were examined at ORNL to characterize their corrosion behavior.

3. EXPOSURE CONDITIONS

Composite tube sections of each type composite were exposed to the industrial waste incinerator for periods of 3, 4, and 6 months (about 2200, 2900, and 4400 h). During this period, the incinerator was reported to have burned a wide range of hazardous and nonhazardous materials including liquid waste from the DuPont Experimental Station Laboratories in Wilmington, Delaware, as well as materials from many other DuPont facilities. The material burned did not include polychlorinated biphenyls (PCBs), dioxin precussors, or radioactive materials, but elemental components of the waste included Na, Ca, P, Si, S, Sb,

Table 1. Designation and constituents of materials exposed to flue gases in a waste incinerator at a maximum temperature of 900°C

Designation in this report	Continuous-filament or strengthening agent	Filament coating	Matrix	Outer coating
166A(x)[a]	PRD166	ZrO_2	Al_2O_3	None
166A/Z(x)	PRD166	ZrO_2	Al_2O_3	ZrO_2
166Z(x)	PRD166	ZrO_2	ZrO_2	None
AS(x)	SiC particles	NA	Al_2O_3	Oxide[b]

[a]x = 3, 4, or 6 to indicate months of exposure.
[b]Aluminosilicate.

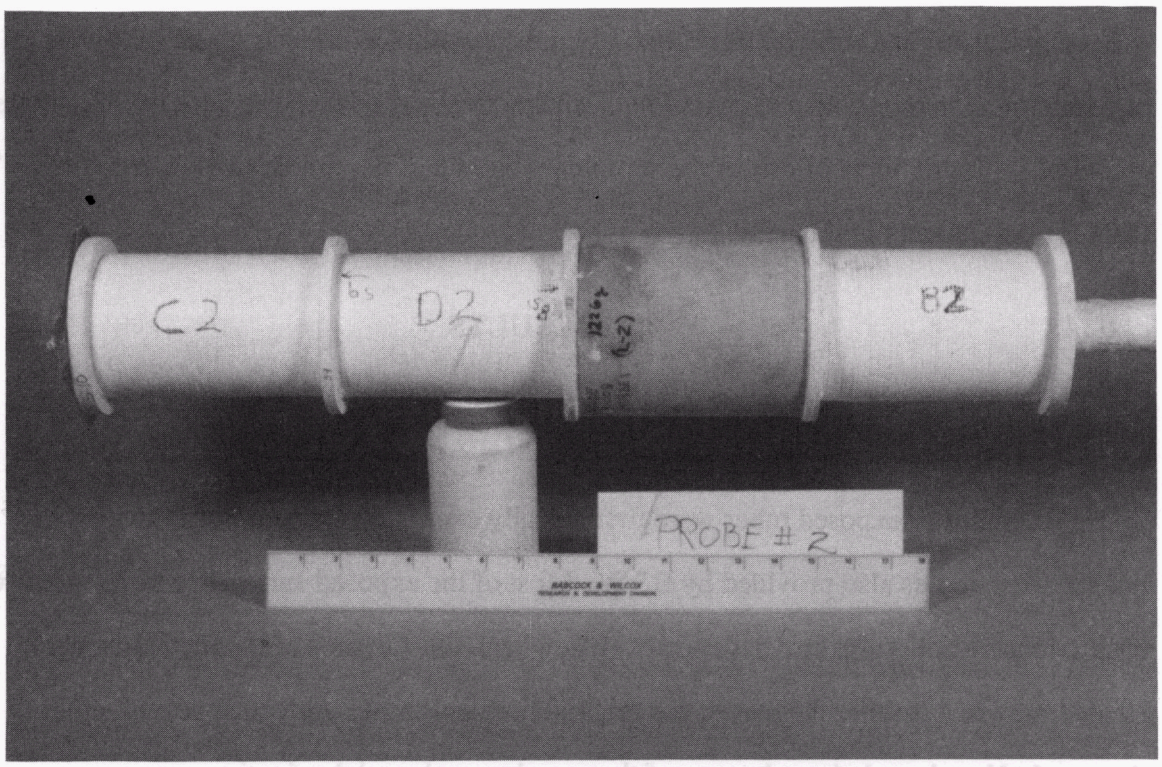

Fig. 1. Before-test sections of as-fabricated ceramic composite tubes that formed a corrosion probe in the waste incinerator. Composite identification, left to right: 166A/Z, 166Z, AS, and 166A. *Source*: Babcock and Wilcox Company, Lynchburg, Virginia.

Fe, Cr, and Ti. After each exposure period, a tube section was removed for strength measurements at B&W and for microstructural examination at ORNL. During the exposure periods, the operating temperature reached about 950°C (1740°F), while the temperature inside the sample tubes reached about 900°C. The incinerator regularly experienced thermal cycles, some down to near-ambient temperature and some down to intermediate temperatures in the range of 250 to 425°C (500 to 800°F). The Inconel tubing was slightly cooled by air flowing through it, and the annulus between the Inconel and ceramic tubes contained lightly packed Saffil fiber insulation to minimize cooling of the ceramic tubes. Impinging flue gases caused deposits and/or discoloration on the outer surfaces of the tubes. The inner surfaces were protected from direct flow of flue gases by zirconia fiber plugs (Fig. 1). Analysis of the flue gases was not determined because of their frequently changing composition associated with different waste charges. However, the principal constituents of the deposits were determined and are discussed in a subsequent section. Figure 2 shows a corrosion probe following an exposure of six months; an accumulation of thicker deposits on some regions of the samples is apparent. Another view of one of the samples is shown in Fig. 3. Corrosion of the alloy 718 plate is also apparent in this view.

4. RESULTS

4.1 VISUAL EXAMINATION

Samples of exposed tubes were first visually examined for comparison with unexposed samples also provided by B&W. Most of the exposed surfaces were covered with rough, loosely adhering, brown deposits. Elsewhere, the surfaces of the materials were stained brown. Neither the matrix nor original filaments at the surface appeared to be damaged. No other obvious damage of the samples, such as delamination, was apparent at this stage of examination.

Fig. 2. A corrosion probe following an exposure of 6 months in the waste incinerator. Discoloration and deposits are apparent. Composite identification, left to right: 166Z(6), 166A(6), AS(6), and 166A/Z(6). *Source*: Babcock and Wilcox Company, Lynchburg, Virginia.

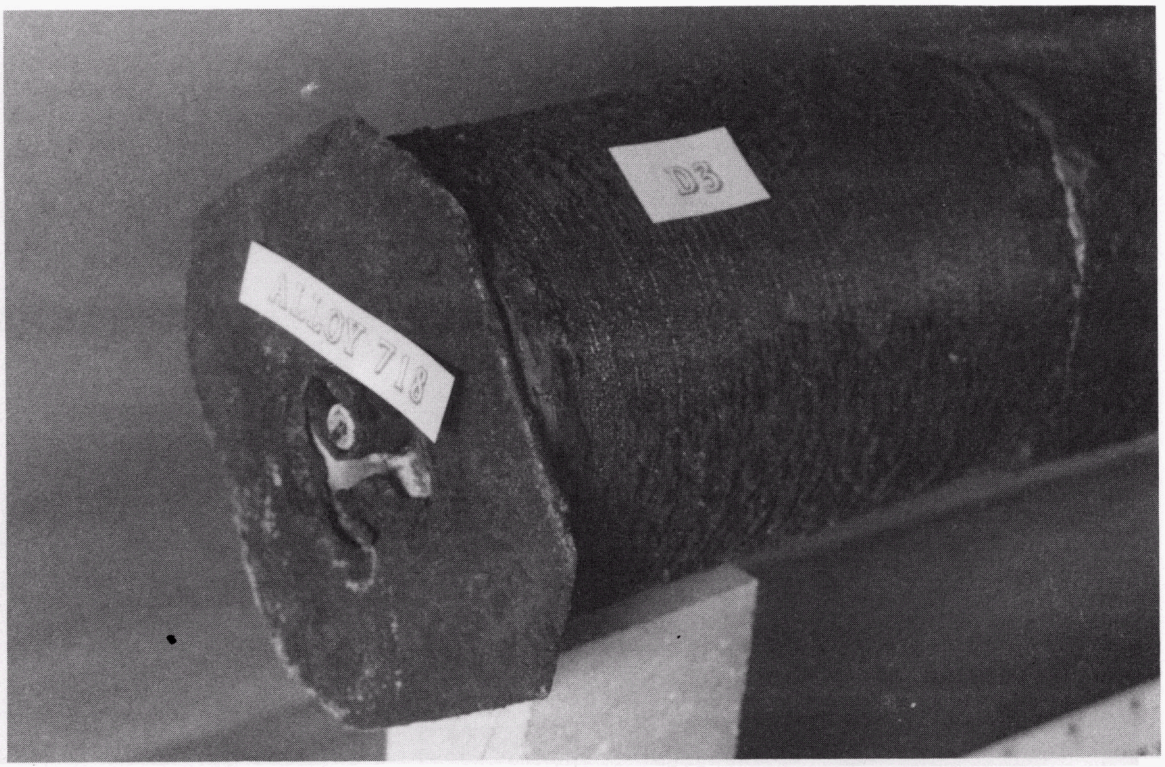

Fig. 3. The zirconia matrix composite, 166Z(6), following an exposure of 6 months in the waste incinerator. The alloy 718 plate, which was pinned to an alloy 600 tube, retained the tube sections during exposure in the incinerator. *Source*: Babcock and Wilcox Company, Lynchburg, Virginia.

4.2 MICROSTRUCTURAL EXAMINATION

Exposed tubes were sectioned by B&W into rings approximately 13 mm (0.5 in.) wide. Segments approximately 19 mm (0.75 in.) long were removed from whole rings to make C-rings for strength measurements. These segments were provided to ORNL for examination of surfaces both parallel and perpendicular to the long axes of the tubes. These were prepared for optical microscopy by polishing to produce smooth, scratch-free surfaces in which the various phases and microstructural features could be observed without chemical etching.

Microstructures of sections of the materials after exposure are shown in Figs. 4 through 7. In general, the continuous-filament composites had a similar appearance, i. e., filaments in a matrix material that contained varying amounts of cracks and pores. A thin deposit or reaction layer is present on the surface of 166A(6) shown in Figs. 4(*a*) and (*b*). Some discoloration was observed in pores of the matrix. The discoloration indicates that very slight attack occurred on the matrix and filaments near the surface. Filaments at or near the surface appear as circles with dark edges as shown in Fig. 4(*c*).

The original zirconia coating that was applied to 166A/Z(6) was not found on the sample shown in Fig. 5; it presumably spalled during one of the many thermal cycles. A thicker deposit (than that shown in Fig. 4) reacted and bonded to this material, but, again, reaction appeared to be slight.

A more extensive reaction layer that was at least partially crystalline in nature occurred on the surface of the 166Z(6) shown in Fig. 6. Filaments near the surface appeared to have reacted to the extent that their identity was lost [Figs. 6(*b*) and (*c*)]. In some cases, part of the filament had been dissolved by the reaction layer, while part remained in an intermediate state of reaction. Other nearby filaments were discolored, suggesting an intermediate state of attack.

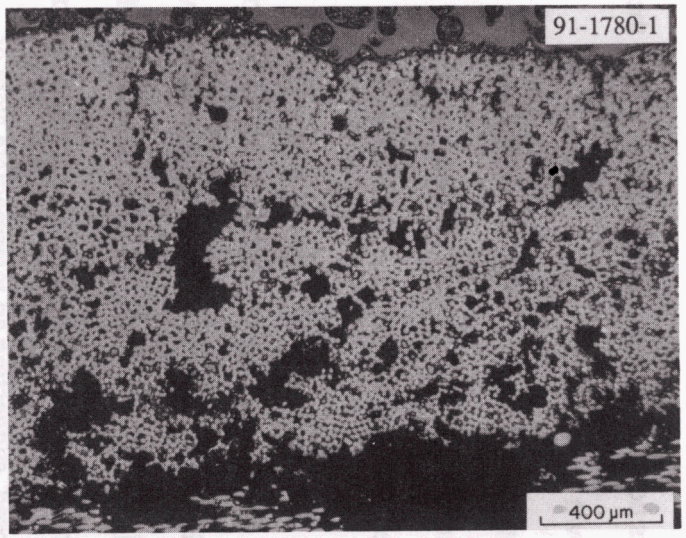

(a)

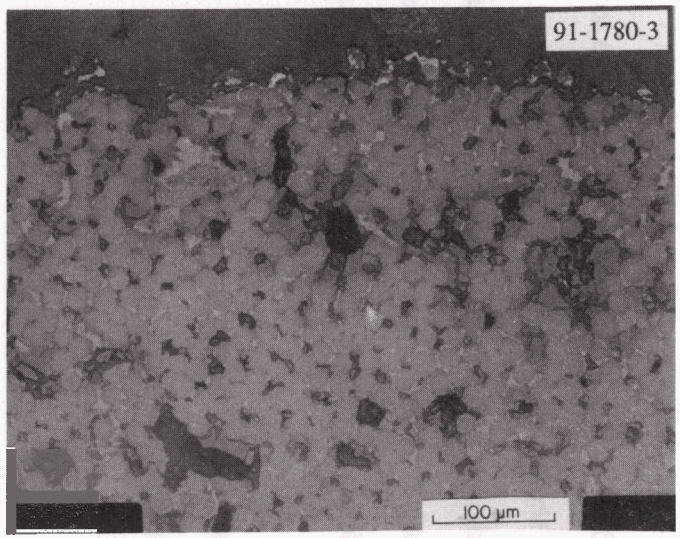

(b)

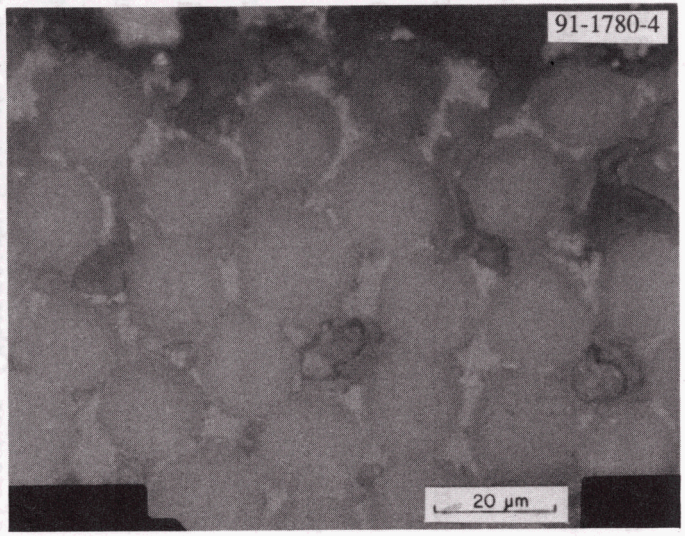

(c)

Fig. 4. Light micrographs of PRD 166/alumina composite [166A(6)] after 6 months' exposure in a hazardous waste incinerator.

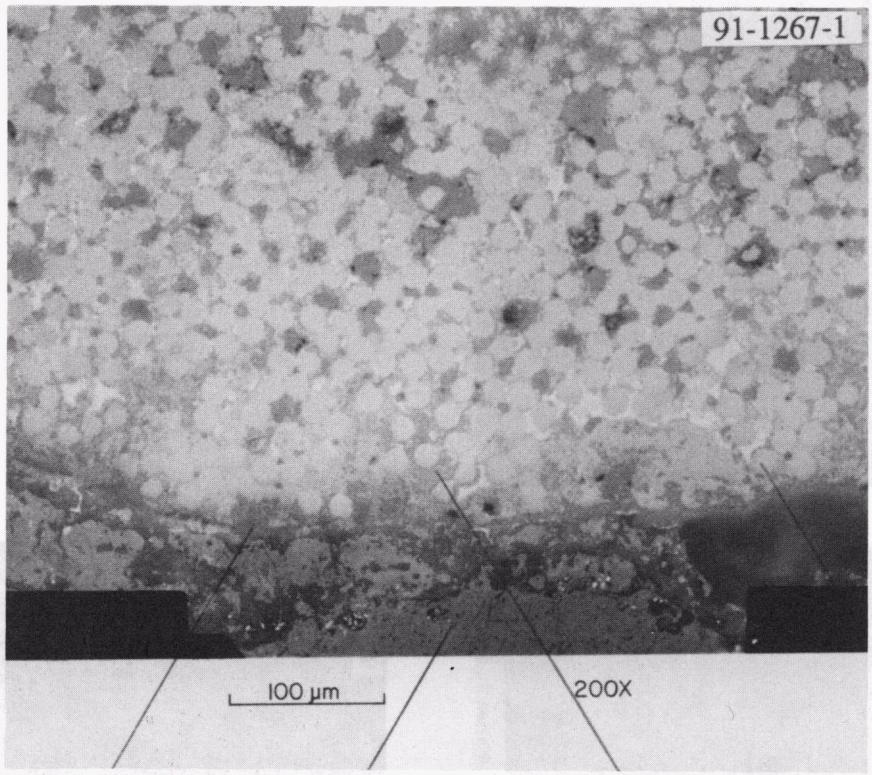

Al_2O_3 matrix ZrO_2 coating

Fig. 5. Light micrograph of PRD 166/alumina composite with a zirconia surface coating [166A/Z(4)] after 4 months' exposure in a hazardous waste incinerator.

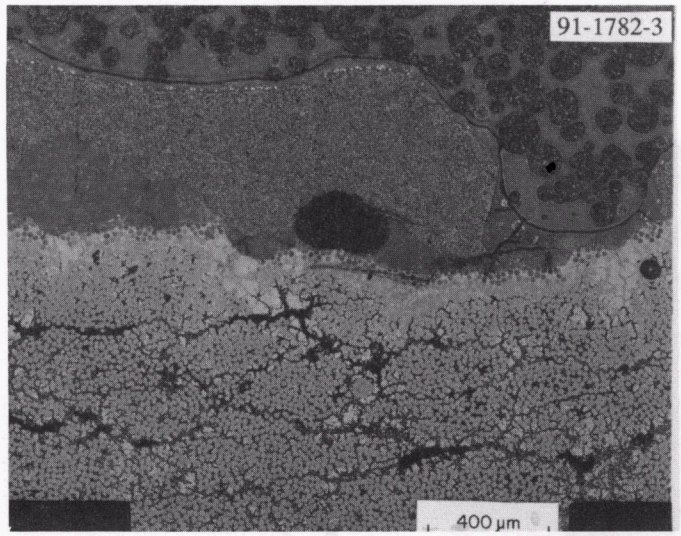

(a)

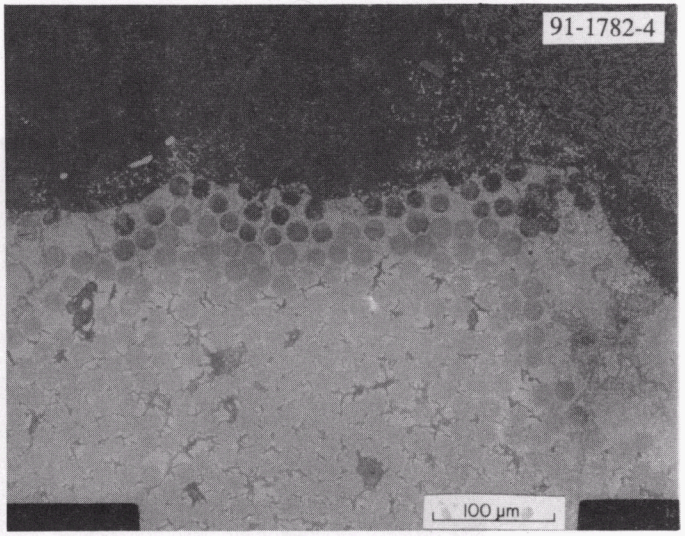

(b)

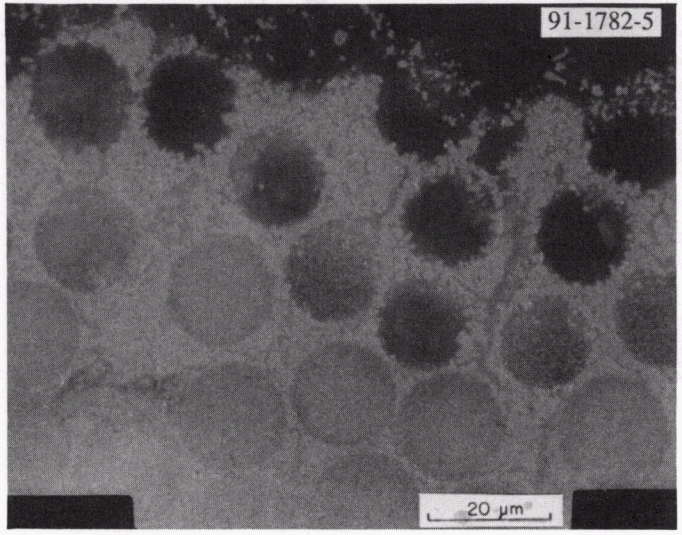

(c)

Fig. 6. Light micrograph of PRD 166/zirconia composite [166Z(6)] after 6 months' exposure in a hazardous waste incinerator.

The AS(6) material in Fig. 7(*a*) also exhibited a thin layer on the surface. The layer contained various phases and was bonded to the original material [Figs. 7(*b*) and (*c*)]. Silicon carbide particles just below the reaction layer were not attacked, as indicated by the angularity of the particles [Fig. 7(*c*)]. The surface layer in Fig. 7 might be a protective oxide coating applied to the surface by the manufacturer or a new layer modified by flue gas constituents. In either case, attack of the parent material appears to be minimal.

4.3 ELECTRON MICROPROBE EXAMINATION

Electron microprobe analysis was used to identify elements in deposits or reaction layers on the surfaces of the composites and to determine the extent of penetration of incineration products into the composites. The following descriptions are based on examination of micrographs produced by back-scattered electrons (BSE) and characteristic X-ray spectra. Light micrographs were also used to aid in interpretation of the microprobe results. Although most of the elements are expected to be present as oxides, the microprobe indicates elemental concentrations only, rather than compounds.

4.3.1 Continuous-Filament Composite with an Alumina Matrix, 166A(x)

Unexposed material is shown in Fig. 8. The BSE image shows the filaments, filament coating, and matrix material. The characteristic X-ray spectra images confirm the alumina matrix, the presence of Al and Zr in the filaments, and the presence of a fragmented zirconia coating on some of the filaments. The same material is shown in Fig. 9 after an exposure of three months in the waste incinerator. The BSE image in Fig. 9(*a*) reveals a deposit on the surface but does not indicate that the material has been significantly attacked. Characteristic X-ray spectra showed that several flue gas constituents (Na, Si, P, and S) had penetrated the microstructure as illustrated by the Na and Si images in Figs. 9(*b*) and (*c*). Elements detected in the deposit were Sb, Na, Si, S, and Fe.

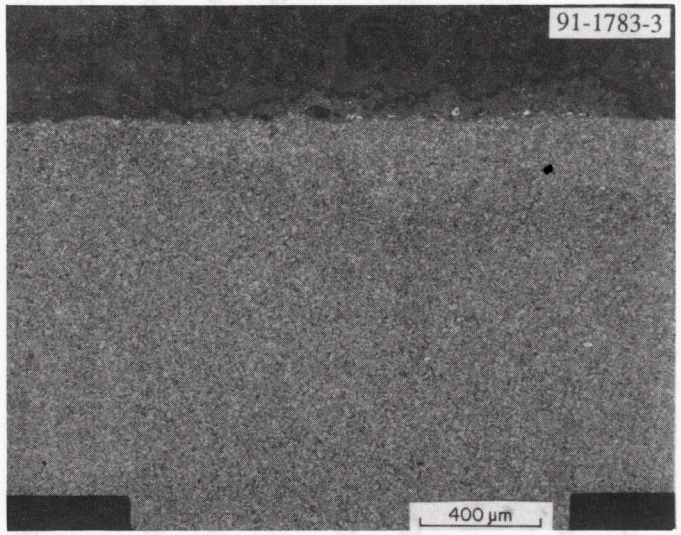

(a)

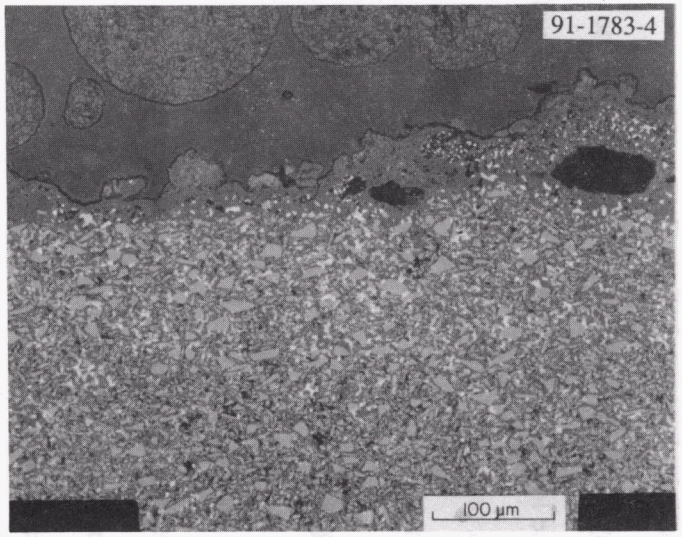

(b)

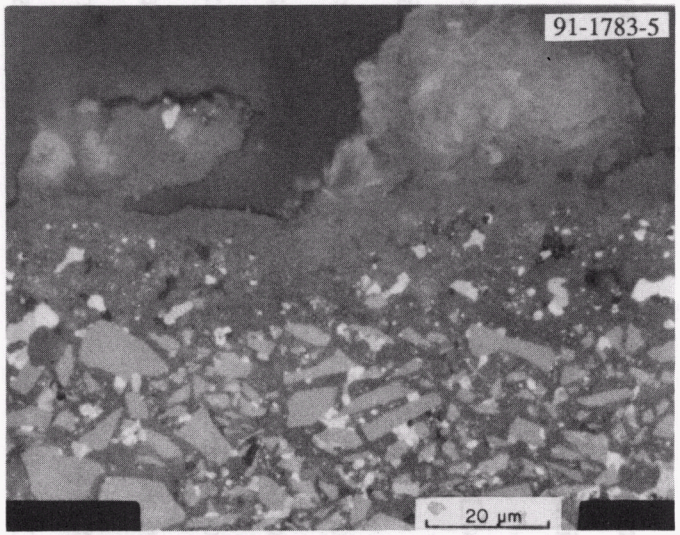

(c)

Fig. 7. Light micrographs of silicon carbide-particulate-strengthened alumina [AS(6)] after 6 months' exposure in a hazardous waste incinerator.

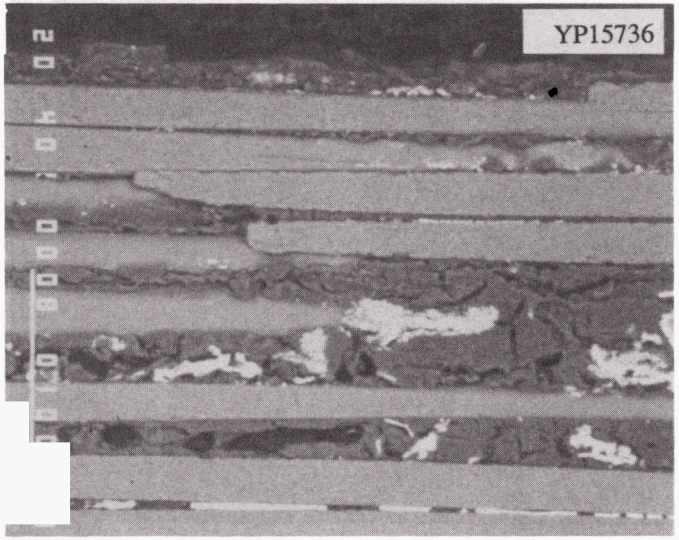

(*a*) BSE

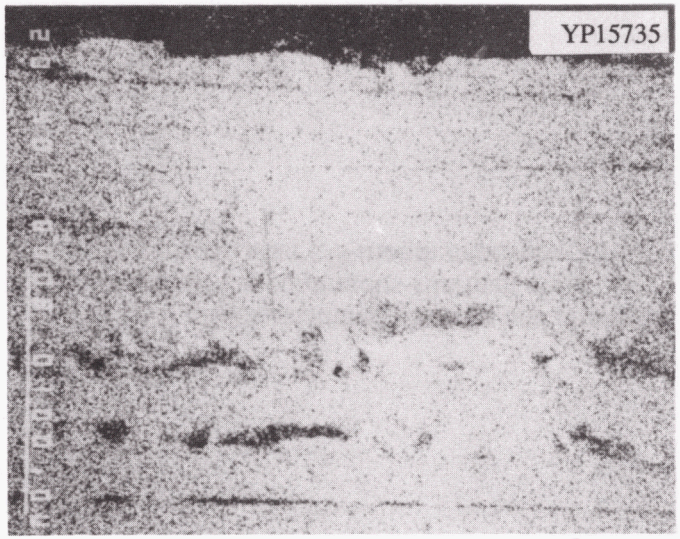

(*b*) Al

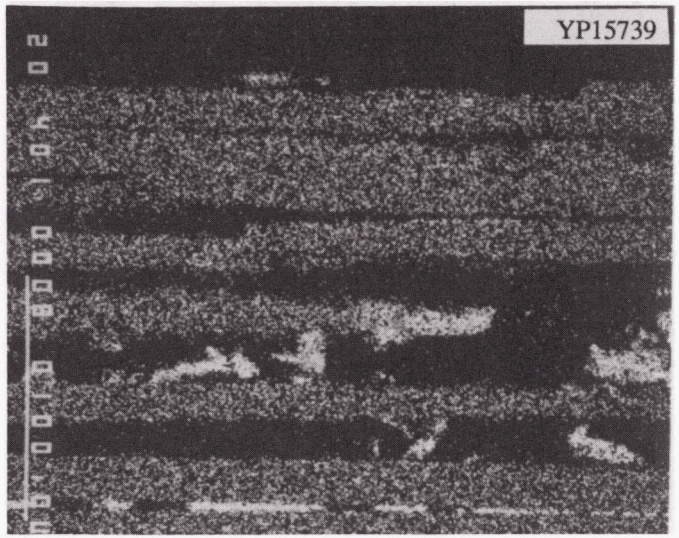

(*c*) Zr

Fig. 8. Back-scattered electron and characteristic X-ray images of the unexposed continuous-filament composite with an alumina matrix [166A(0)].

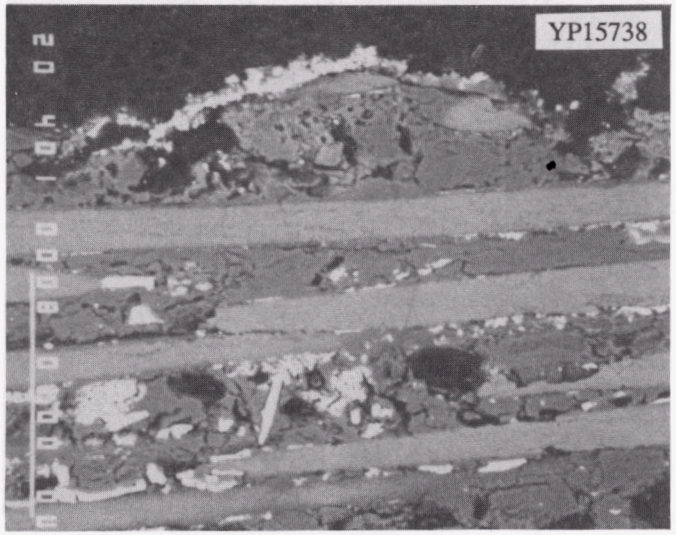

(*a*) BSE

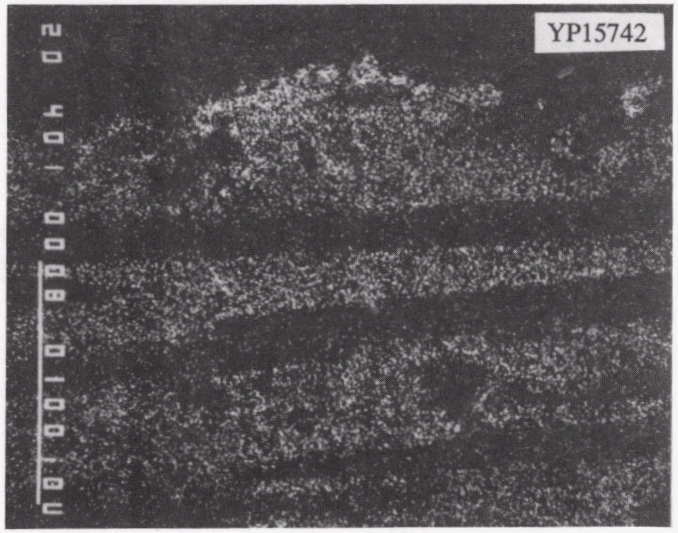

(*b*) Na

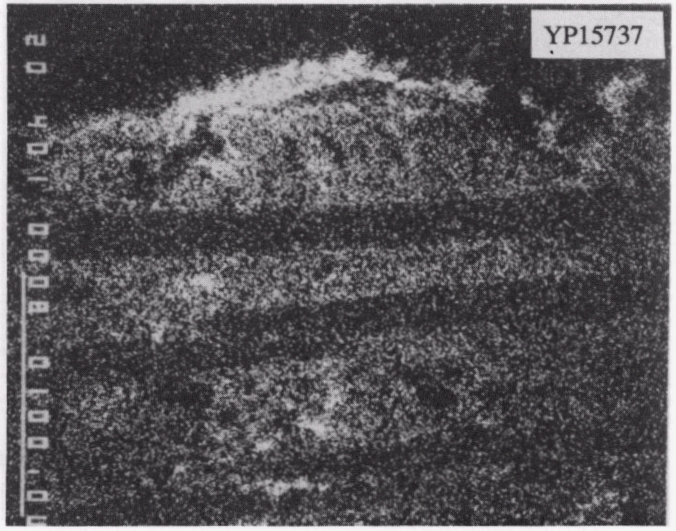

(*c*) Si

Fig. 9. Back-scattered electron and characteristic X-ray images of the continuous-filament composite with an alumina matrix after a 3-month exposure [166A(3)].

After an exposure of four months, the BSE image in Fig. 10(*a*) still does not indicate that the material has undergone chemical attack. As before, Na and S were detected in the alumina matrix [Figs. 10(*b*) and (*c*)], and small regions containing Na, Ca, Cr, Fe, and S were identified in the matrix.

After an exposure of 6 months, the BSE image in Fig. 11(*a*) reveals neither a deposit nor evidence of reaction, except for dark surfaces on filaments near the surface (shown as a dark edge on the circular cross section). A zirconia coating, the bright material surrounding some filaments, is clearly evident in Fig. 11(*a*), while the presence of Al in the matrix and filaments is confirmed in Fig. 11(*b*). Again, Na was found in the matrix [Fig. 11(*c*)]; however, the concentration, relative to an exposure of 4 months, could not be quantified. The presence of Fe, K, P, and Sn in the matrix was also indicated, and isolated small regions on the surface contained Ca, Fe, and Sn. Sodium, K, and S were also detected at the midpoint of the wall thickness, indicating that these elements had migrated at least approximately 1.5 mm through the matrix.

In order to further characterize the microstructure of composite 166A, the most prominent elements in the matrix and filaments were identified with the electron microprobe. These were Al, Ca, P, Si, and Zr. Other elements, including Fe, Na, S, Sb, and Ti, were present in relatively smaller amounts. The five predominant elements were quantitatively determined at various locations as described in Table 2. The elemental concentrations were converted to oxides, and the results were normalized to provide analyses at various sites. The absolute accuracy of the measurements in Table 2 is less important than the concentration differences or other insights revealed by the data.

Several important microstructural and compositional features can be identified from Fig. 12 and Table 2. A fragmented ZrO_2 coating (88 to 98 wt % ZrO_2) was present on some filaments. Analyses of the centers of filaments at the surface, and at least 2 mm from the surface, revealed an Al_2O_3/ZrO_2 ratio between 3:1 and 4:1, which corresponds well to a

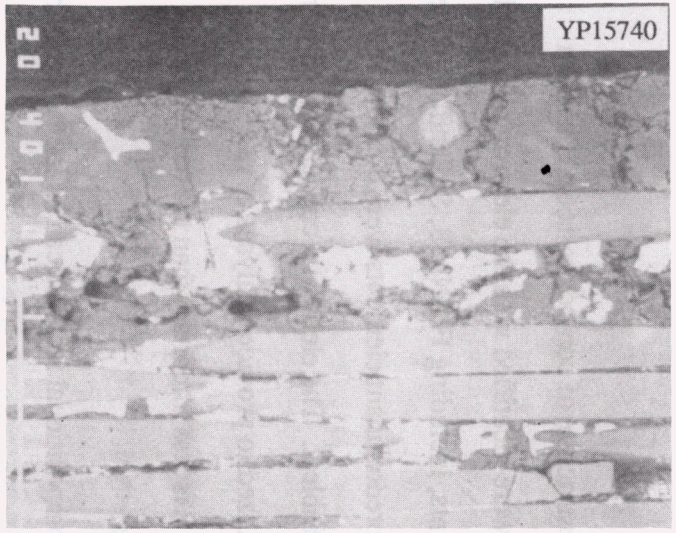

(*a*) BSE

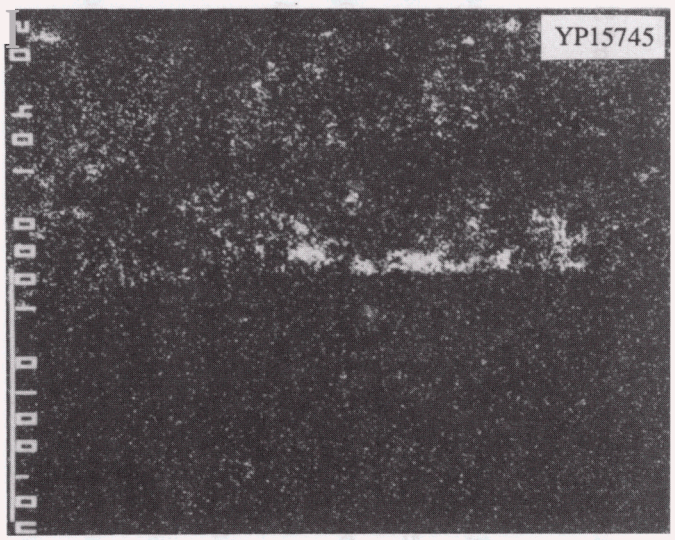

(*b*) Na

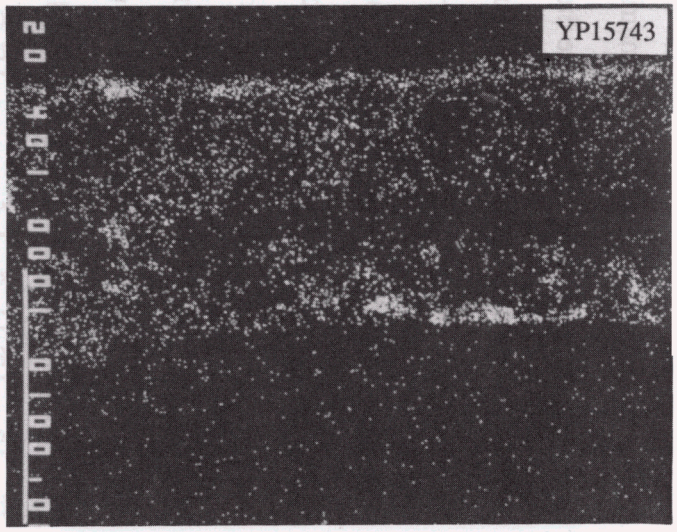

(*c*) S

Fig. 10. Back-scattered electron and characteristic X-ray images of the continuous-filament composite with an alumina matrix after a 4-month exposure [166A(4)].

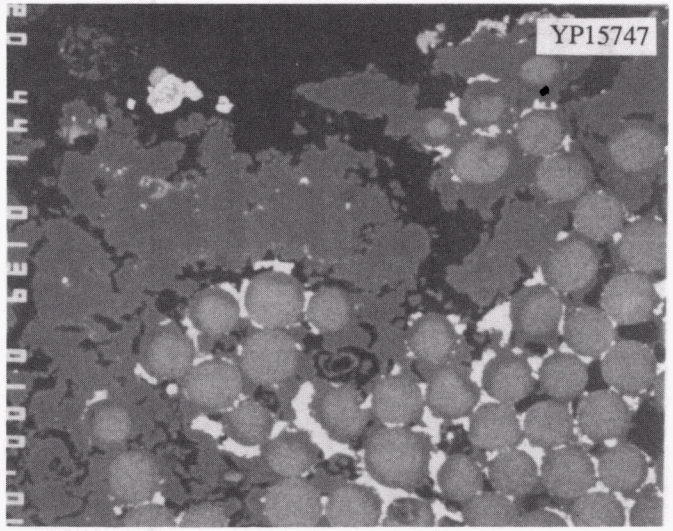

(*a*) BSE

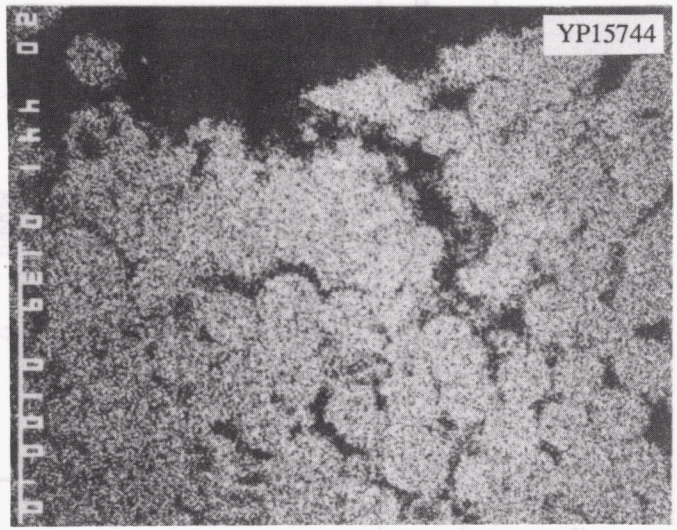

(*b*) Al

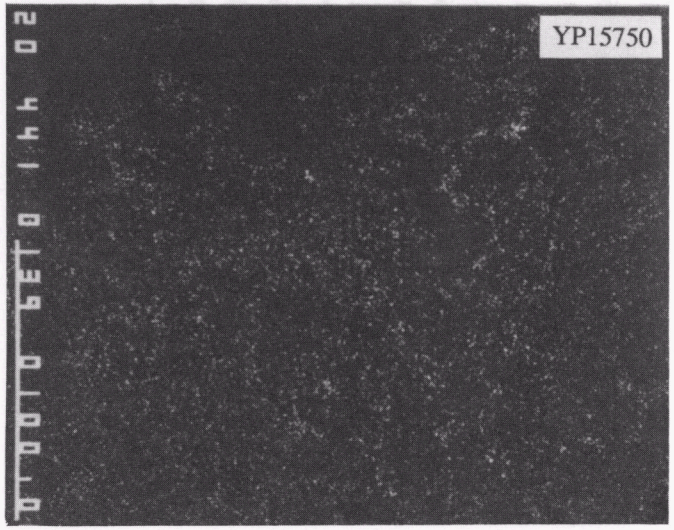

(*c*) Na

Fig. 11. Back-scattered electron and characteristic X-ray images of the continuous-filament composite with an alumina matrix after a 6-month exposure [166A(6)].

Table 2. Concentration at various sites within composite 166A(6)

Depth (mm)	Concentration wt %					Location of analysis site
	Al_2O_3	CaO	P_2O_5	SiO_2	ZrO_2	
0	74	0	1	1	25	center of filament
	93	0	2	2	3	dark edge of filament
	1	0	1	1	98	coating on filament
≈0.1	82	1	8	10	0	matrix
	73	0	0	1	26	center of filament
	92	0	3	4	0	matrix
	97	0	1	1	0	matrix
≈1	75	0	2	1	22	center of filament
	96	0	3	1	0	matrix
	92	0	5	2	0	matrix
	10	0	1	1	88	coating on filament
	87	1	6	3	4	dark edge of filament
	80	0	1	1	17	center of filament
≈2	78	0	1	0	21	center of filament
	1	0	1	0	98	coating on filament
	92	0	6	1	1	matrix
	1	46	53	0	0	between filaments
	1	47	51	0	1	between filaments
	91	1	7	2	0	matrix
	33	31	36	0	0	between filaments
	93	0	4	1	1	matrix
	87	1	9	3	0	matrix

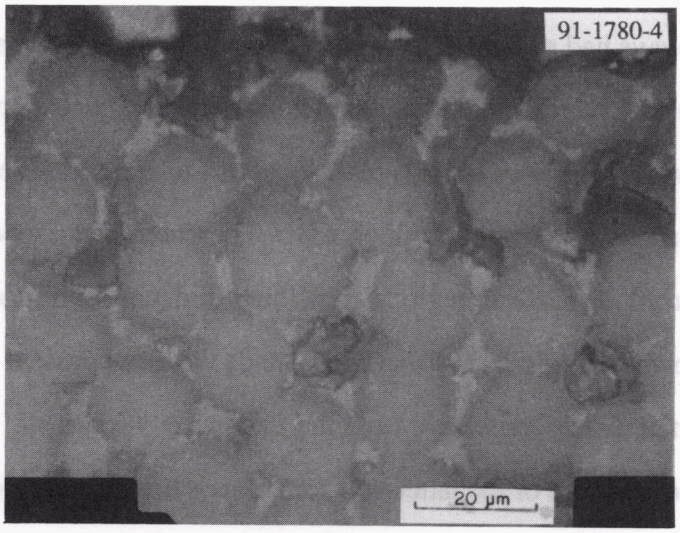

(*a*)

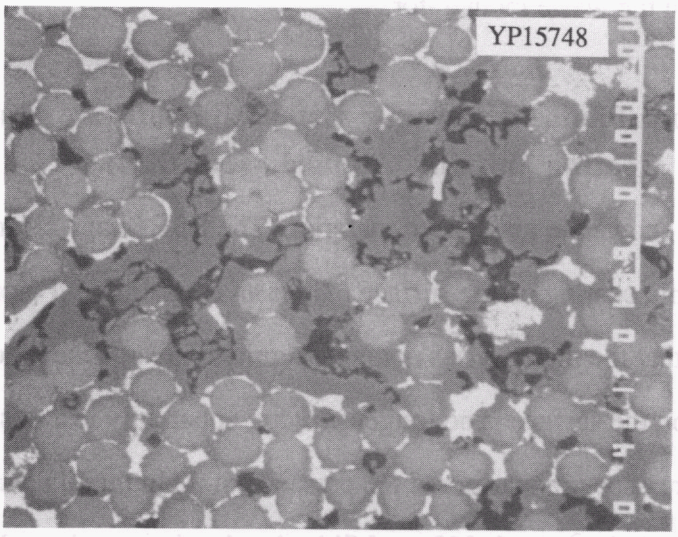

(*b*)

Fig. 12. Light micrographs of composite 166A(6) showing locations where electron microprobe semiquantitative elemental measurements were made.

filament composition of Al_2O_3-20 mole % ZrO_2. Filaments, especially near the surface, had dark edges that always had substantially lower concentrations of ZrO_2 as shown in Table 2, but filaments with dark edges and corresponding low ZrO_2 contents occurred to a depth of at least 1 mm. Figure 12(*b*) shows other typical locations where measurements were made. The matrix material always contained a high Al_2O_3 content as was expected. At three locations, 2 mm from the surface, regions containing high concentrations of CaO and P_2O_5 were found as shown in Table 2. If these compounds were not present in the original composite, then their source must have been the flue gas environment.

Neither the presence of the latter two compounds nor the variation in composition from the center to the dark edge of filaments can be readily explained; however, these compositional variations do not seem to indicate that substantial degradation of the composite occurred during exposure in the waste incinerator.

4.3.2 Continuous-Filament Ceramic Composite with an Alumina Matrix Zirconia Coating Initially Applied, 166A/Z(x)

Figure 13 shows the unexposed material. The BSE image clearly shows the filaments, matrix, and zirconia coating on the surface. After an exposure of 4 months, the BSE image in Fig. 14 indicates that the material has not been significantly attacked; however, the original zirconia coating on the surface is no longer present, apparently lost to spallation. Characteristic X-ray spectra confirmed the presence of Al in the filaments and matrix, and Zr in the filaments, and also revealed Na and Si in the alumina matrix and the presence of Na, Si, S, Fe, and Ca in a thin layer on the surface. After 6 months, the BSE photograph in Fig. 15 shows no evidence of the zirconia coating on the surface but also no evidence of a deposit or reaction layer on the surface. Sodium was distributed in the alumina matrix, and Fe and Sn were present in a thin layer on the surface. Thus, the electron microprobe examination revealed little or no attack on the material in agreement with the optical micrograph in Fig. 5.

(*a*) BSE

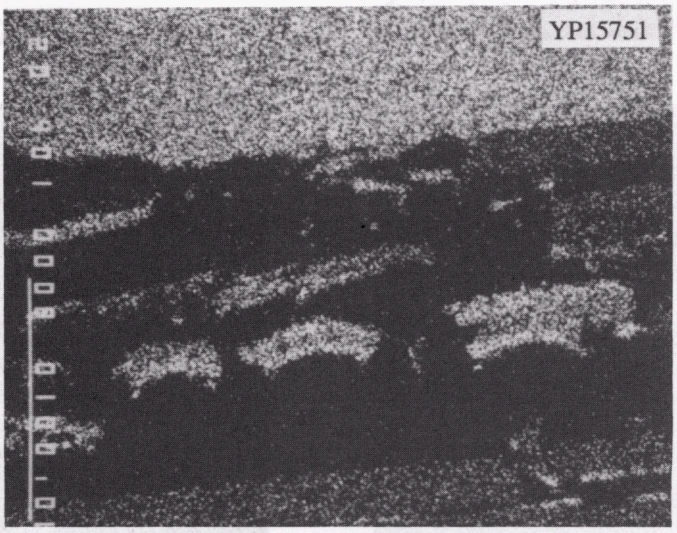

(*b*) Zr

Fig. 13. Back-scattered electron and characteristic X-ray images of the unexposed continuous-filament composite with an alumina matrix and zirconia surface coating [166A/Z(0)].

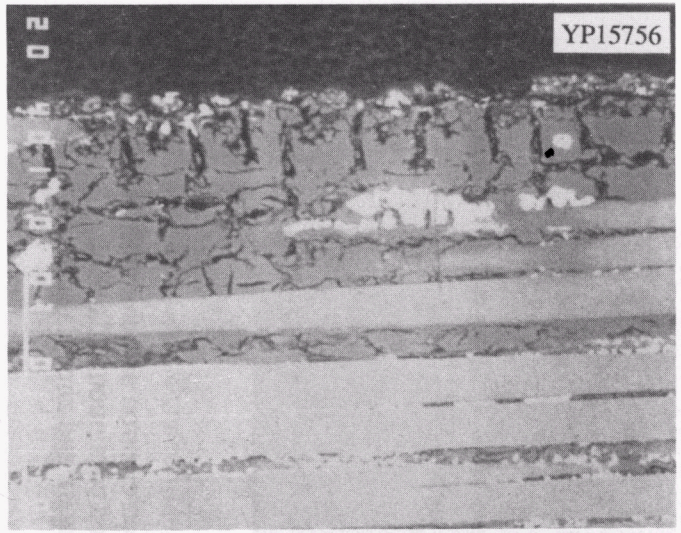

(*a*) BSE

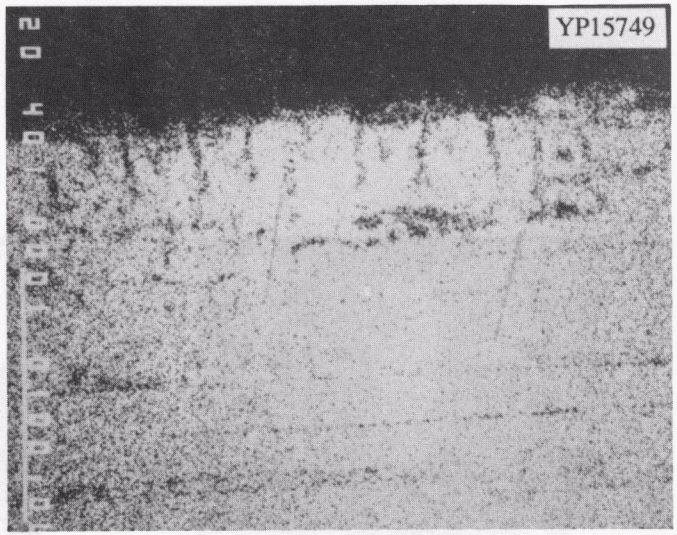

(*b*) Al

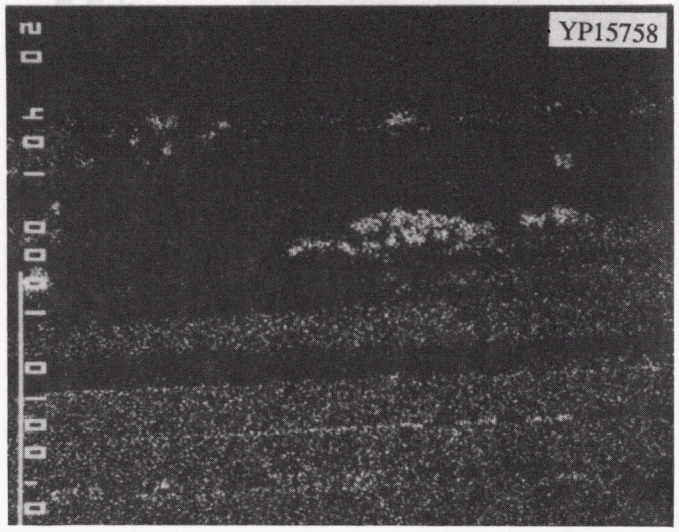

(*c*) Zr

Fig. 14. Back-scattered electron and characteristic X-ray images of the continuous-filament composite with an alumina matrix and zirconia surface coating after an exposure of 4 months [166A/Z(4)].

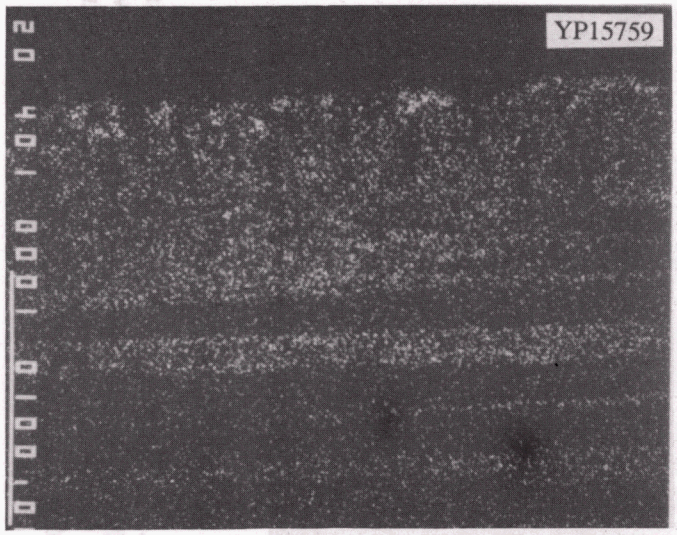

(*d*) Na

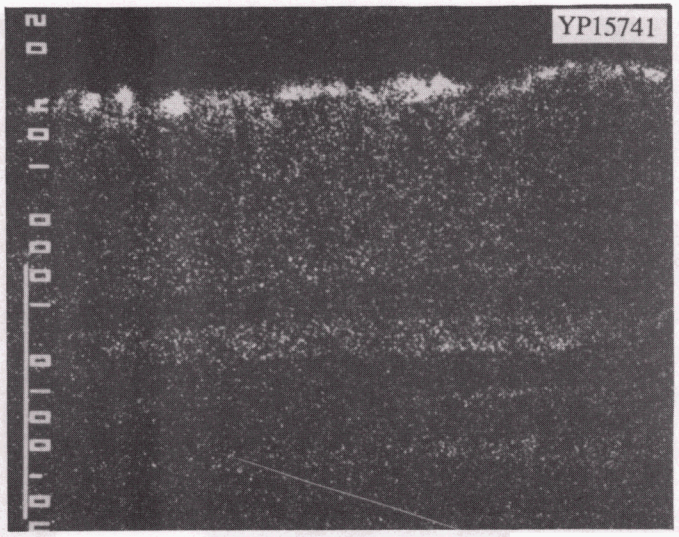

(*e*) Si

Fig. 14. (Continued)

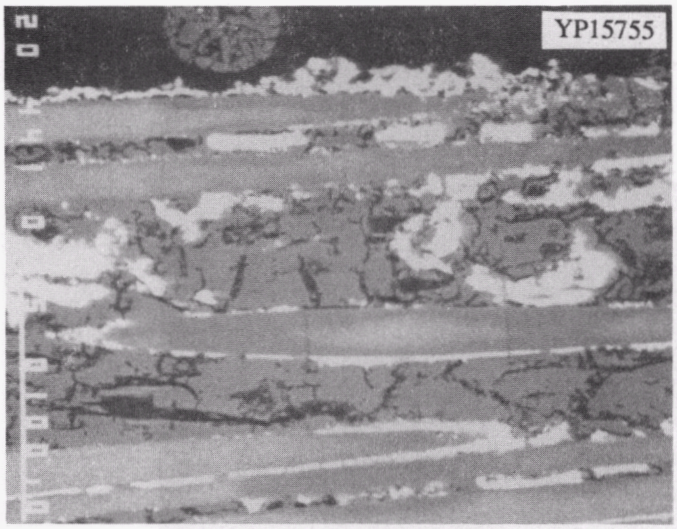

(*a*) BSE

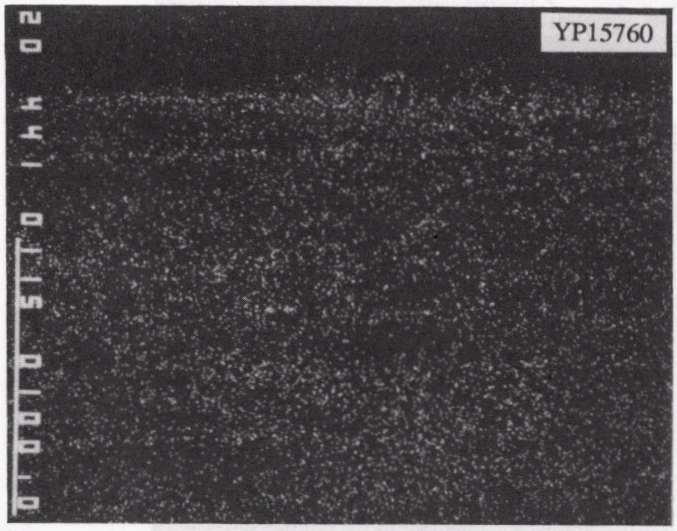

(*b*) Na

Fig. 15. Back-scattered electron and characteristic X-ray images of the continuous-filament composite with an alumina matrix and zirconia surface coating after an exposure of 6 months [166A/Z(6)].

4.3.3 Continuous-Filament Ceramic Composite with a Partially Stabilized Zirconia Matrix, 166Z(x)

The unexposed material is shown by the BSE image and characteristic X-ray spectra in Fig. 16. After 3 months, the BSE image in Fig. 17 shows a deposit on the surface; however, the filaments and matrix do not exhibit evidence of attack at this time. The deposit contained substantial concentrations of Al, Na, Si, S, P, and Ca (as illustrated for Na, Si, and S in Fig. 17). Phosphorus was especially concentrated in cracks near the surface. Silicon, Na, and Ca were detected in the matrix. The BSE image after 4 months, in Fig. 18, indicates that a reaction with the matrix has occurred because regions with a high concentration of Al are present in what should be the zirconia matrix. Sodium, however, is still mostly present in the surface layer. After 6 months' exposure in the incinerator, the BSE photograph in Fig. 19 reveals two distinct reaction layers. (None of the original composite material is shown in this view.) The outer layer contained crystalline-like material in a glassy matrix, while the inner layer consisted of elongated grains in a matrix material. The outer layer had substantial concentrations of Al, Na, S, and Si, and, possibly, Sb and Sn. Calcium and Mg were present in both layers. The enlongated grains in the inner layer may be alumina or a mixture of aluminosilicates, e. g. mullite and/or sodium aluminosilicate compounds; however, this possibility was not confirmed by analysis. Isolated particles in the inner layer contained high concentrations of Ca, while isolated regions at the interface between the two layers contained Fe and Ti.

Figure 20 reveals that the filaments near the surface were severely attacked in this material in contrast to the behavior of composite 166A and 166A/Z. The BSE image in Fig. 20(*a*) shows that filaments at or near the surface have completely reacted and that others are in an intermediate stage of reaction. Reacted filaments have lower Al and Zr contents but higher Ca, Na, P, and Si, as shown by the characteristic X-ray spectra in Figs. 20(*b*–*g*). Elemental concentrations were obtained at specific sites as in the case of composite 166A(6).

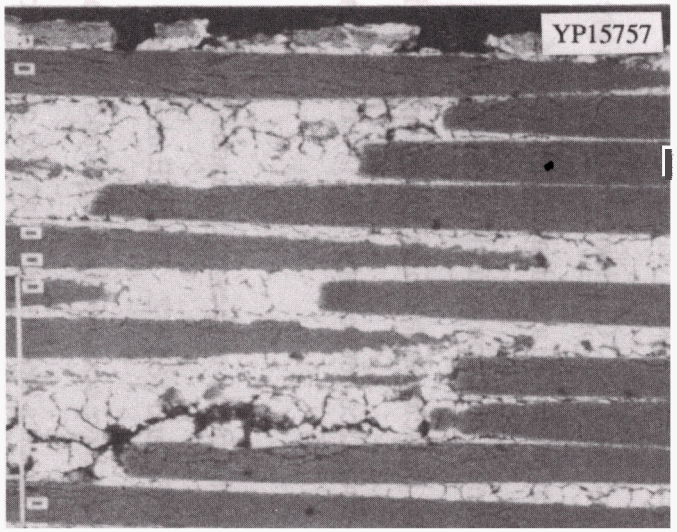

(*a*) BSE

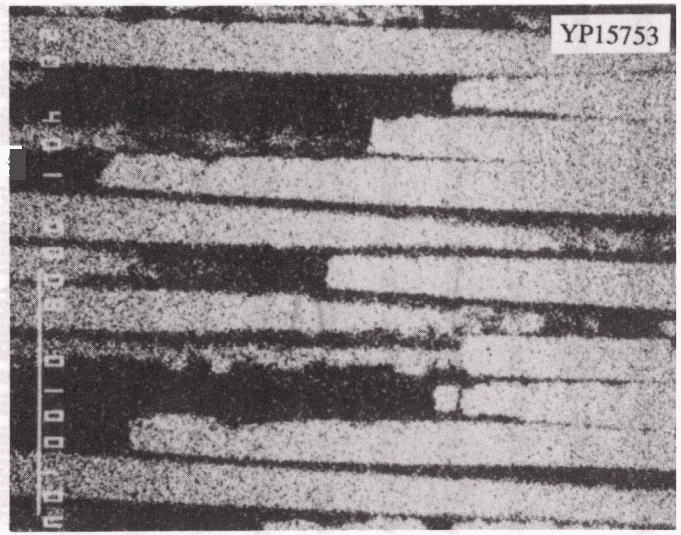

(*b*) Al

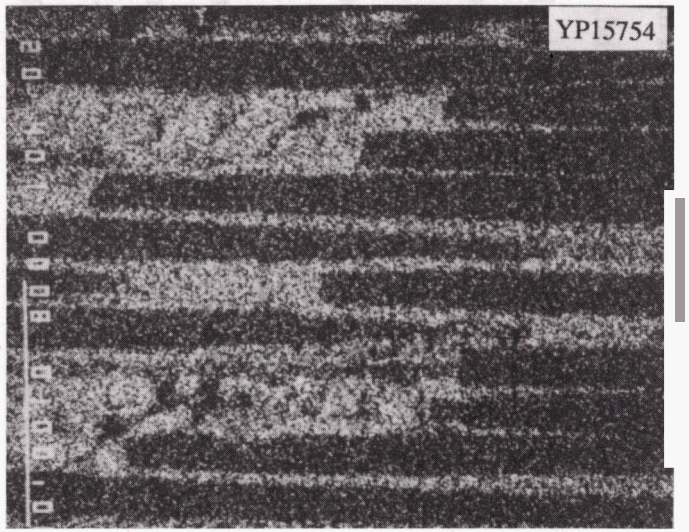

(*c*) Zr

Fig. 16. Back-scattered electron and characteristic X-ray images of the unexposed continuous-filament composite with a zirconia matrix [166Z(0)].

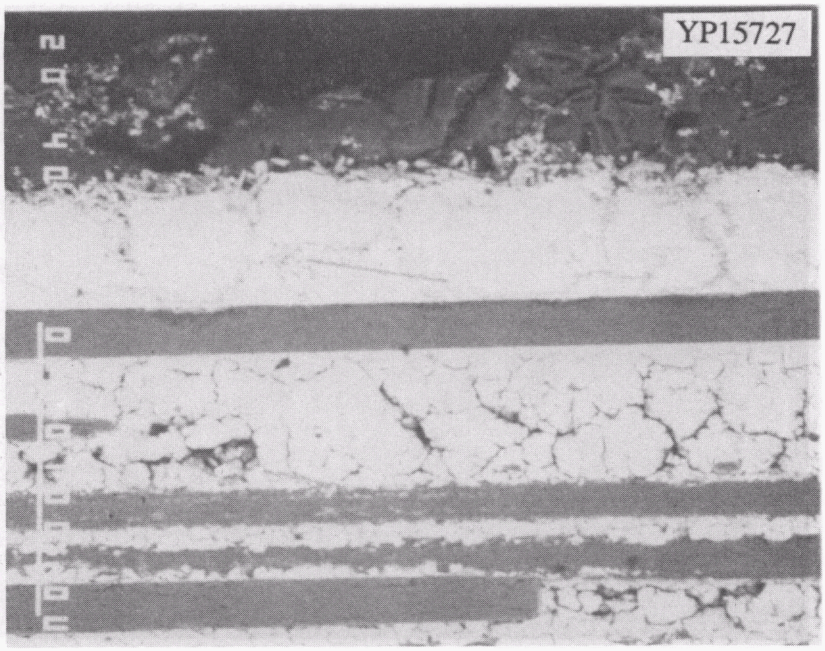

(*a*) BSE

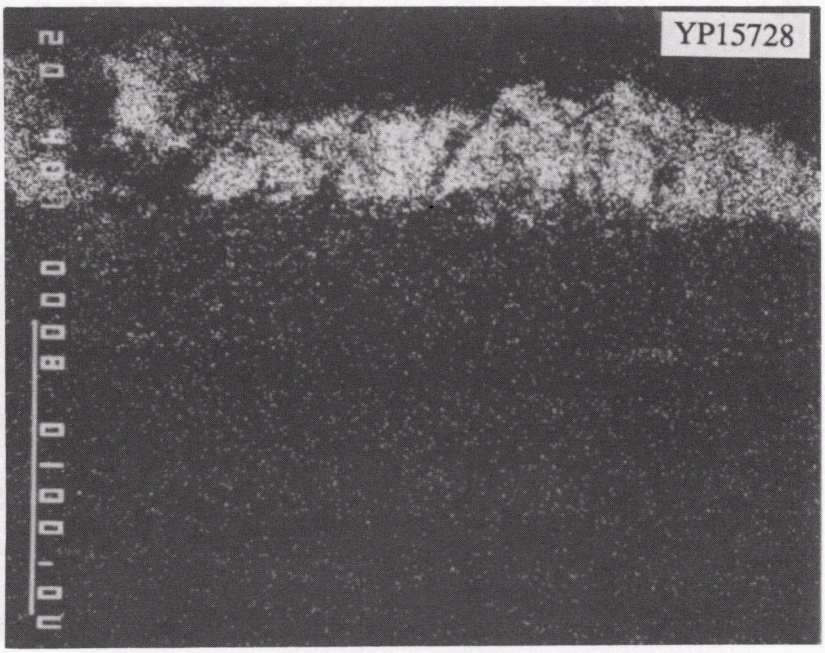

(*b*) Na

Fig. 17. Back-scattered electron and characteristic X-ray images of the continuous-filament composite with a zirconia matrix after an exposure of 3 months [166Z(3)].

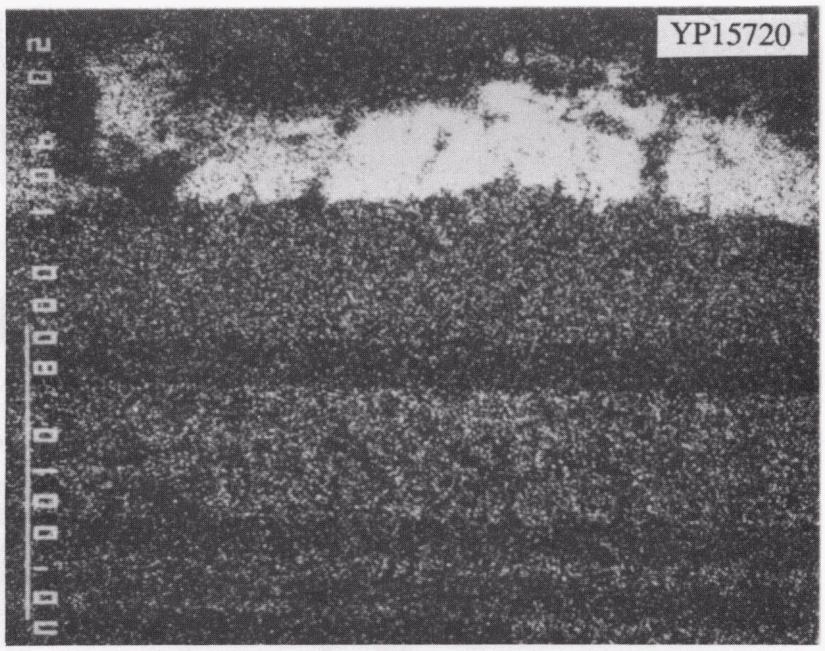

(*c*) Si

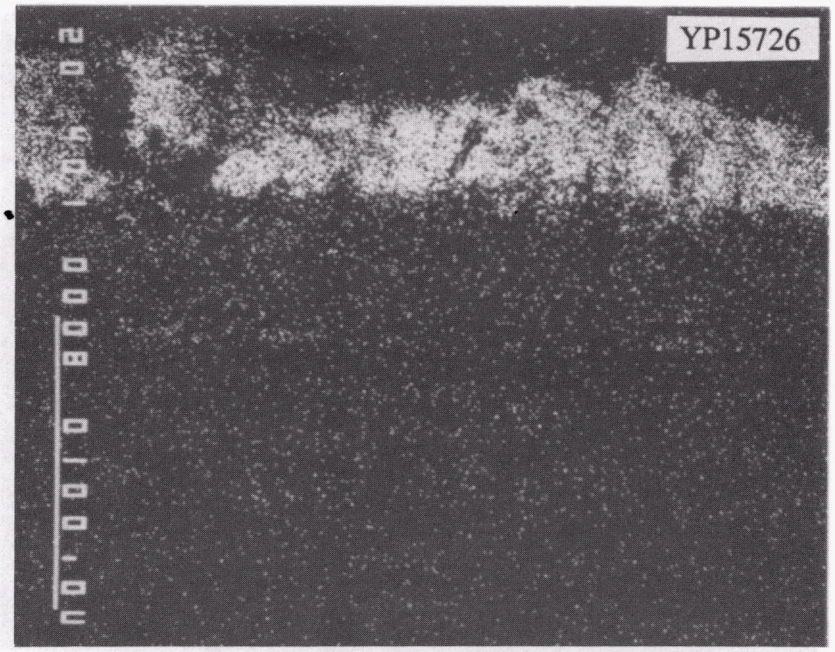

(d) S

Fig. 17. (continued)

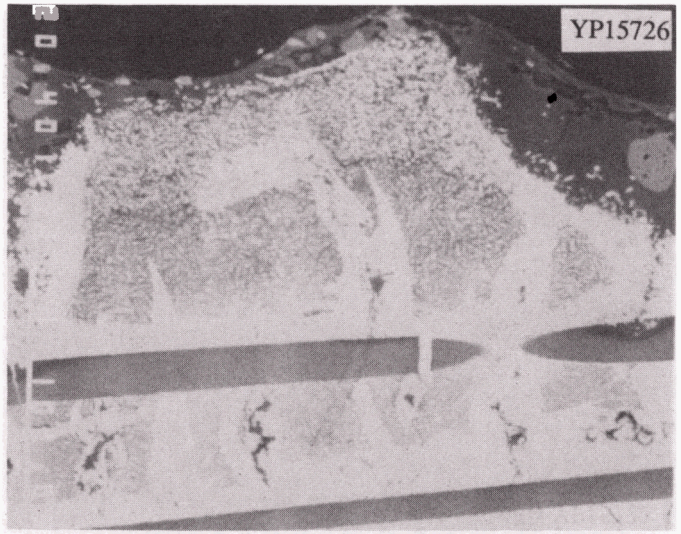

(*a*) BSE

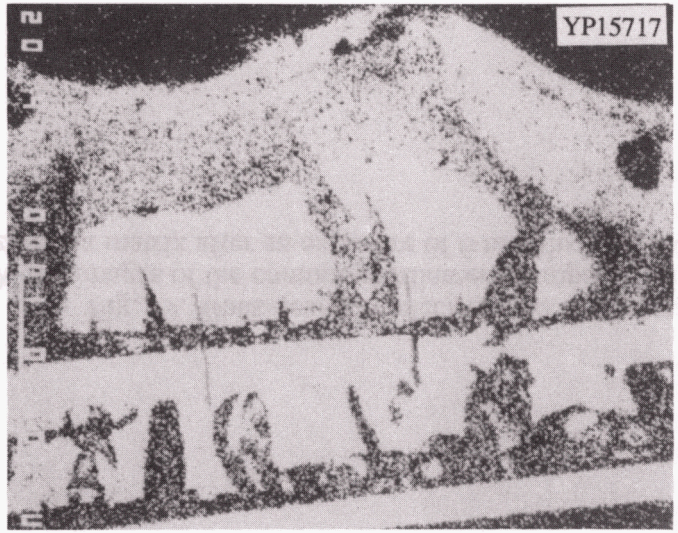

(*b*) Al

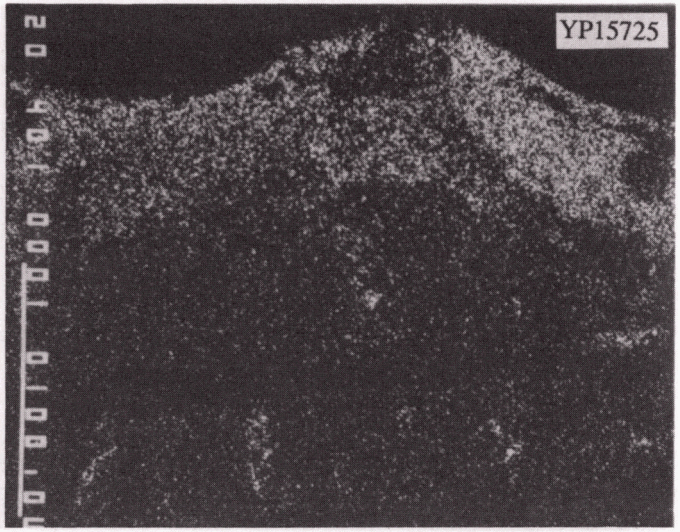

(*c*) Na

Fig. 18. Back-scattered electron and characteristic X-ray images of the continuous-filament composite with a zirconia *matrix* after an exposure of 4 months [166Z(4)].

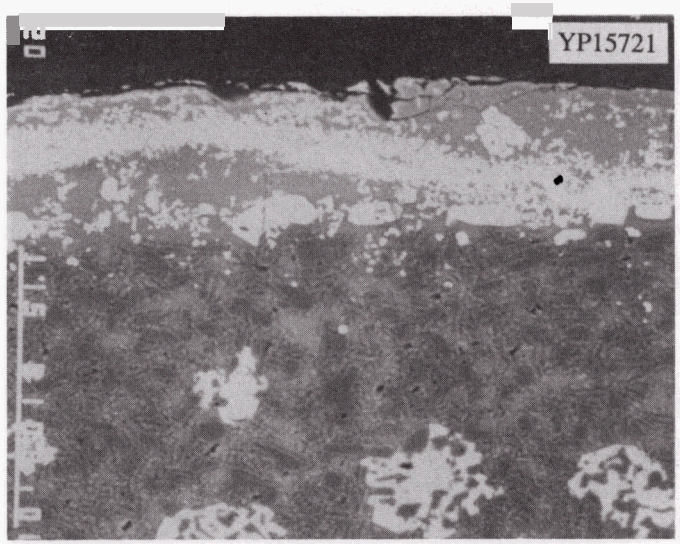

(*a*) BSE

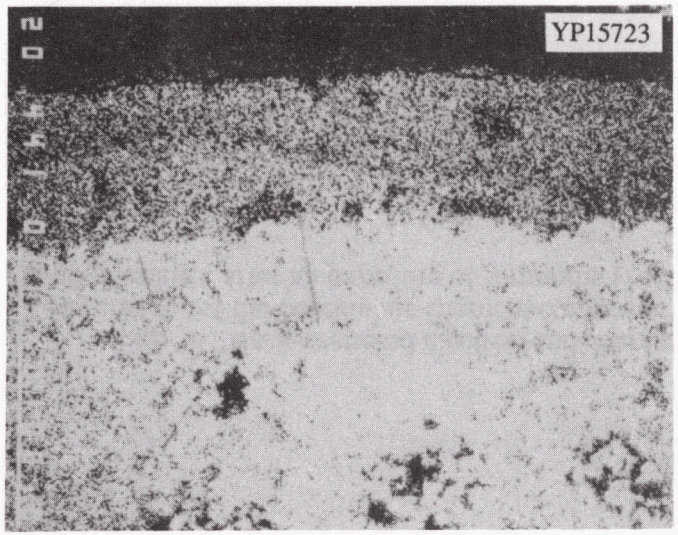

(*b*) Al

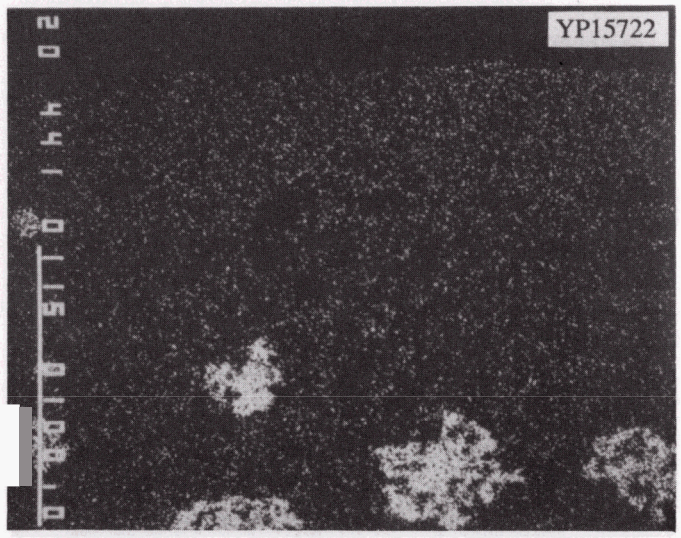

(*c*) Ca

Fig. 19. Back-scattered electron and characteristic X-ray images of the continuous-filament composite with a zirconia matrix after an exposure of 6 months [166Z(6)].

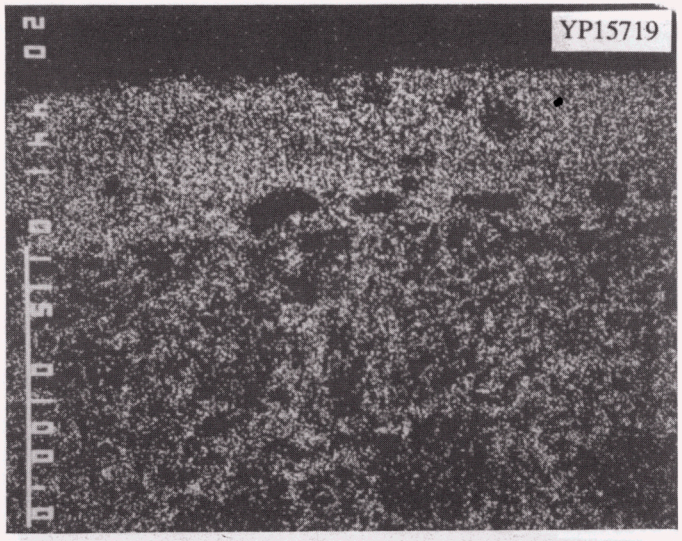

(*d*) Na

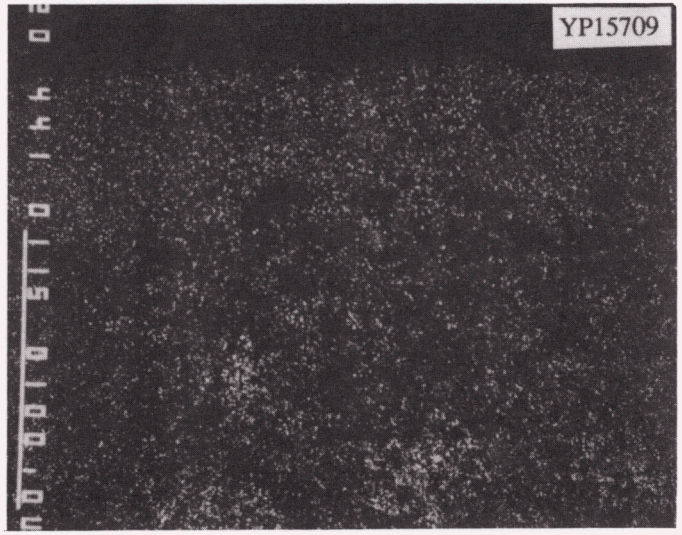

(*e*) S

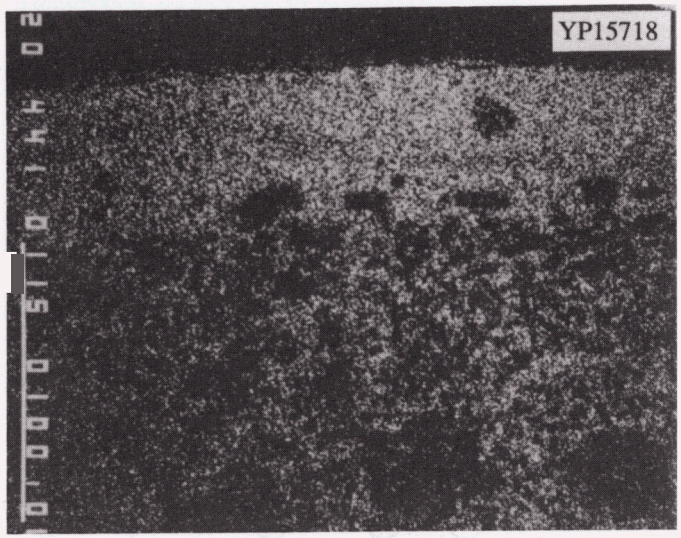

(*f*) Si

Fig. 19. (continued)

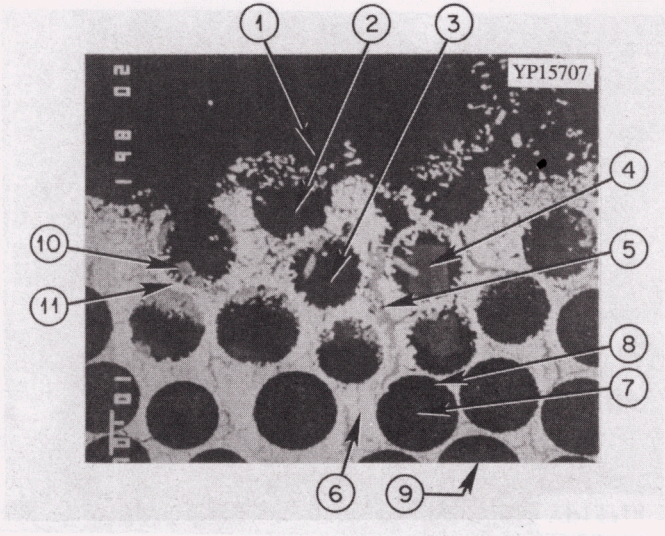

(*a*) BSE

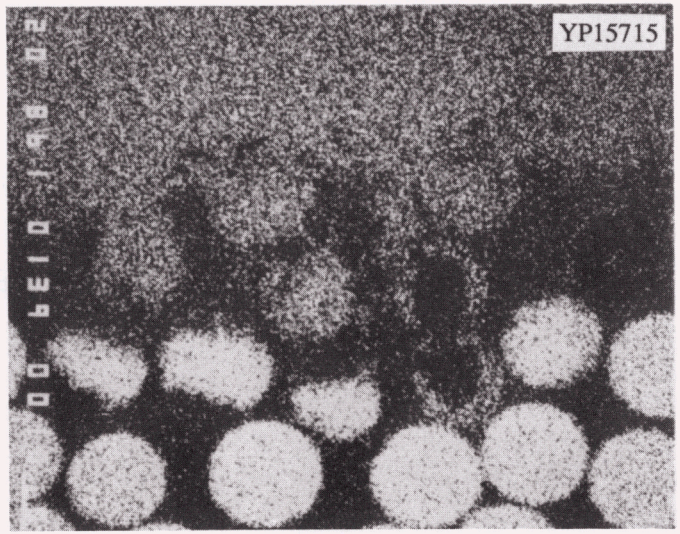

(*b*) Al

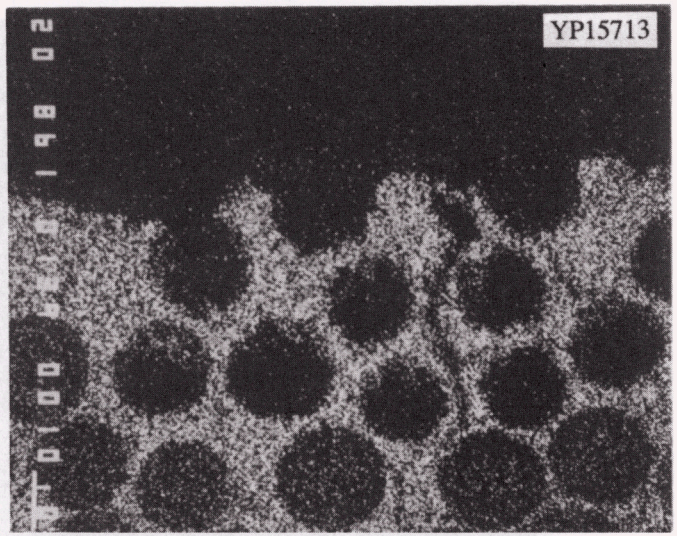

(*c*) Zr

Fig. 20. Back-scattered electron and characteristic X-ray images of sample 166Z(6) showing locations where electron microprobe semiquantitative elemental measurements were made.

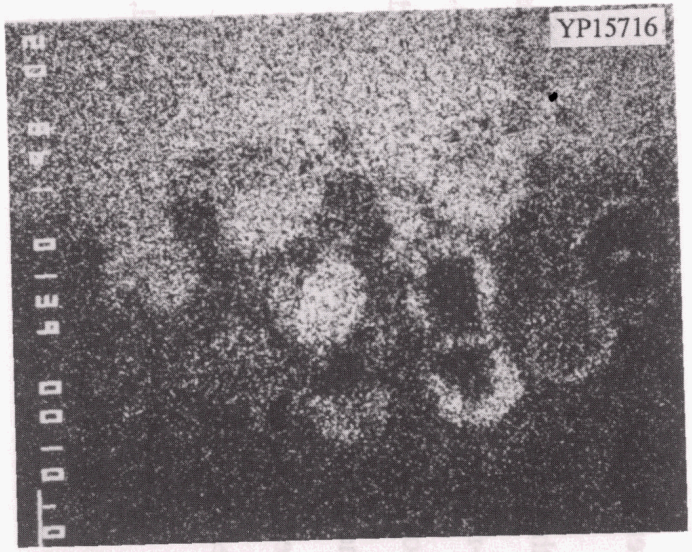

(*d*) Si

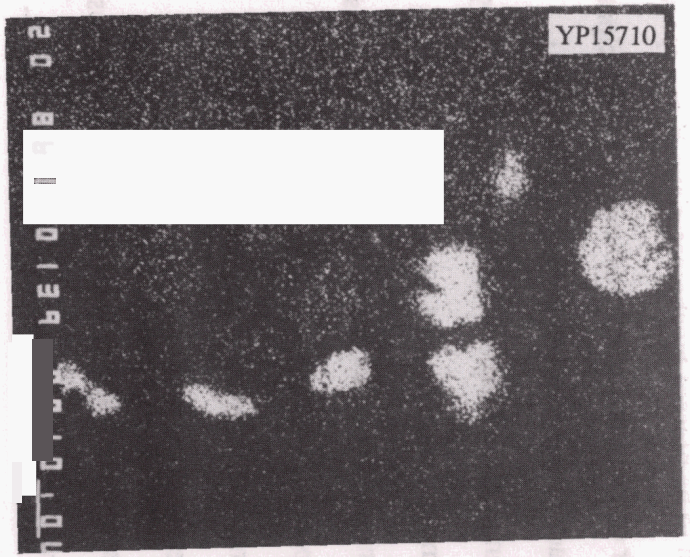

(*e*) Ca

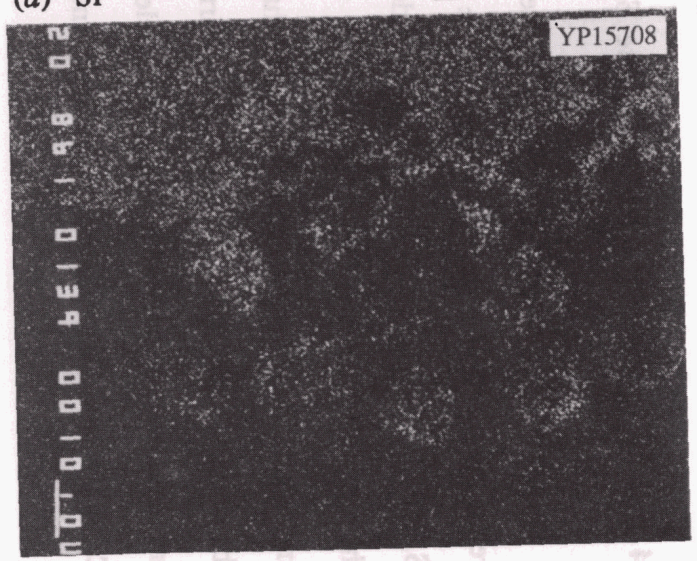

(*f*) Na

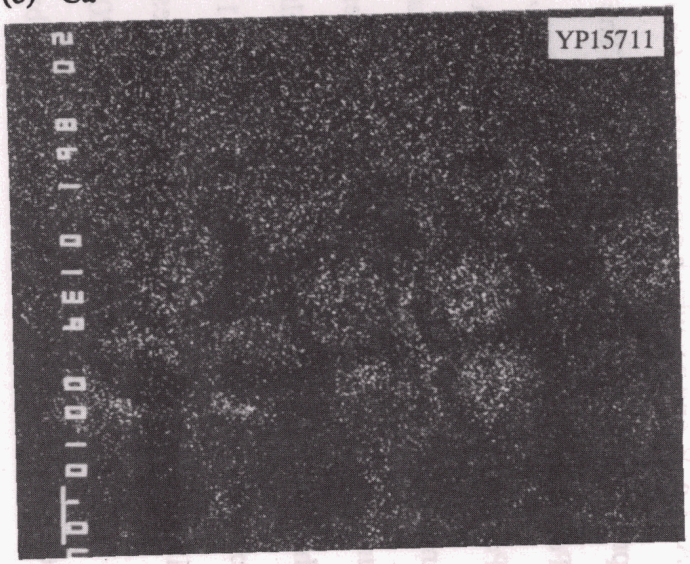

(*g*) P

Fig. 20. (continued)

Table 3 shows that the reaction layer on the surface (point 1) contained high concentrations of Al, Ca, P, and Si, which along with Na (shown to be present by characteristic X-ray spectra), probably is a complex silicate material. The Zr content, however, was lower than anticipated. Points 2 and 3, the sites of reacted filaments, had compositions similar to that in point 1. Point 4 reveals Ca and P had displaced the Al and Zr in a filament near the surface. Point 5 indicates a concentration of P in a crack in the matrix, while point 6 represents a relatively uncontaminated matrix. Points 7 and 9 represent unreacted filaments, while point 8 reveals the low Zr concentration along the edge of filaments as was noted in filaments near the exposed surface of 166A(6). Points 10 and 11 represent crystal formation in a reacted filament and slightly contaminated matrix, respectively, near the exposed surface.

The photographs (Figs. 16 through 20) and data (Table 3) clearly show that composite 166Z was much more extensively corroded by high-temperature flue gases than was 166A. Later in this report, the possible cause of this behavior will be addressed.

4.3.4 Alumina Matrix Composite Strengthened with Silicon Carbide Particles, AS(x)

The BSE image in Fig. 21, taken after three months' exposure, reveals a deposit or reaction layer on the surface. Characteristic X-ray spectra showed the presence of Al, Na, Si, S, and Ca in the layer. After 6 months, the deposit or reaction layer was definitely bonded to the original material as shown in Fig. 22(*a*). The deposit or reaction layer (top) contained crystals, voids of various sizes, and cracks that extended into the the original material (bottom). Characteristic X-ray spectra confirmed the presence of Al in the matrix of the original material and Si in the original particles. The deposit or reaction layer contained Al, Ca, Na, S, and Si, while the crystals contained Ca, Fe, P, and Zr.

Table 3. Analysis of various regions at or near the surface of composite 166Z(6)[a]

Point	Concentration wt %					Location of analysis site
	Al_2O_3	CaO	P_2O_5	SiO_2	ZrO_2	
1	29	6	33	30	2	reaction layer
2	27	5	35	32	2	reacted filament
3	31	4	33	31	2	reacted filament
4	0	74	26	0	0	crystal in reacted filament
5	1	9	76	1	14	crack in matrix
6	1	0	3	0	95	matrix
7	73	0	1	2	24	center of filament
8	88	1	3	4	4	edge of filament
9	77	0	0	1	22	center of filament
10	17	5	50	12	16	crystal in reacted filament
11	3	2	2	3	90	matrix

[a]Analysis points are shown in Fig. 20(*a*).

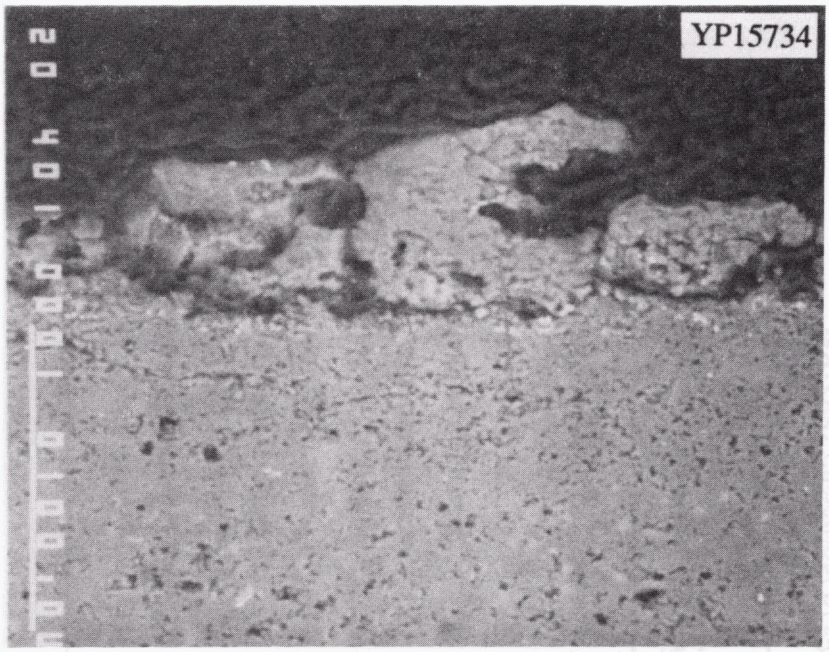

(*a*) BSE

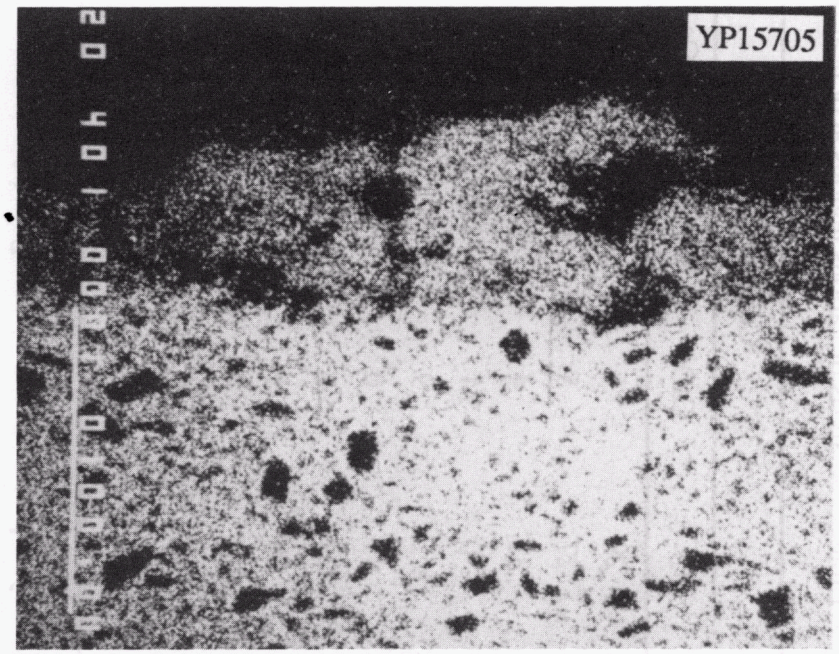

(*b*) Al

Fig. 21. Back-scattered electron and characteristic X-ray images of the silicon carbide-particulate-strengthened alumina composite after an exposure of 3 months [AS(3)].

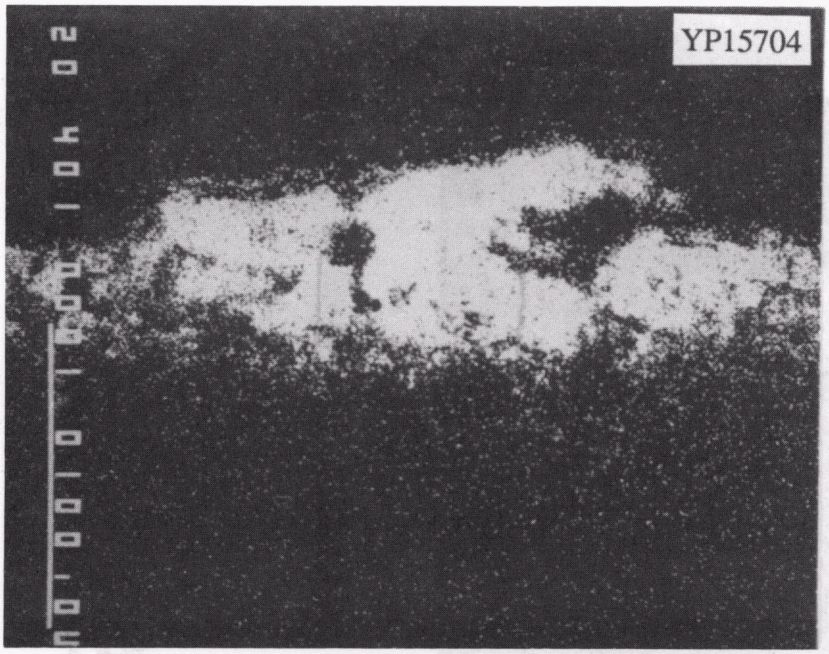

(*c*) Na

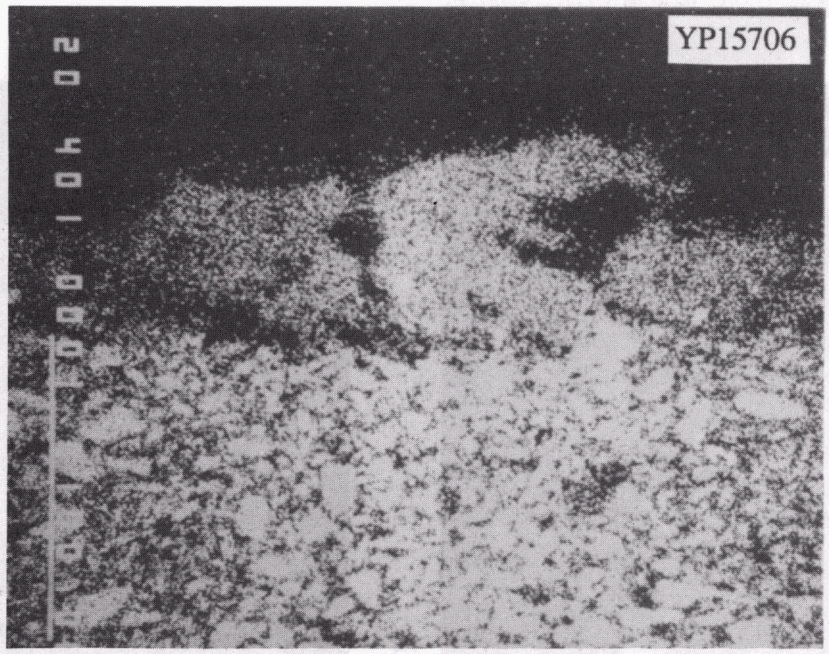

(*d*) Si

Fig. 21. (continued)

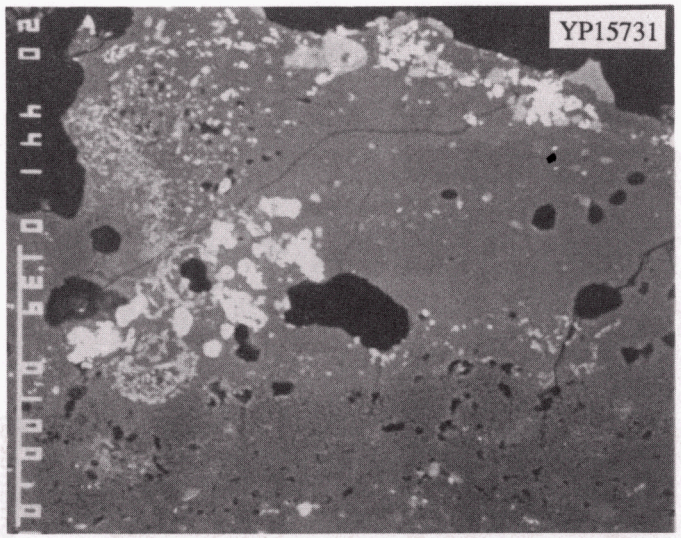

(*a*) BSE

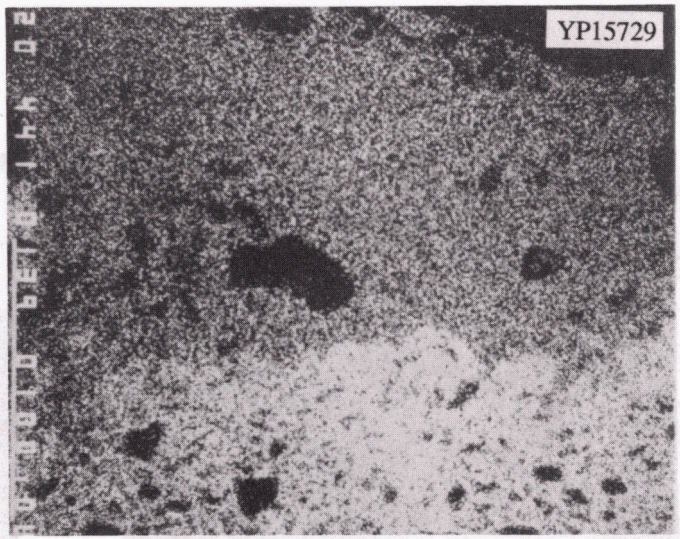

(*b*) Al

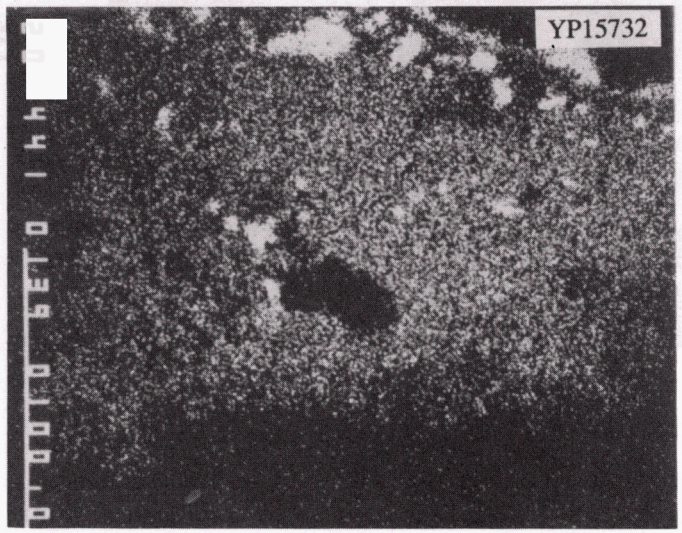

(*c*) Ca

Fig. 22. Back-scattered electron and characteristic X-ray images of the silicon carbide-particulate-strengthened alumina composite after an exposure of 6 months [AS(6)].

5. DISCUSSION AND CONCLUSIONS

Three types of ceramic composite materials were exposed to flue gases in a hazardous waste incinerator to assess their suitability for heat exchanger tubes. One composite consisted of continuous filaments of PRD-166 (Al_2O_3-20 wt % ZrO_2) in an alumina matrix, with and without a zirconia coating on the outer surface (designated 166A and 166A/Z). Another composite consisted of PRD-166 filaments in a zirconia matrix (166Z), and the third type of composite was a commercially available material having an alumina matrix strengthened with silicon carbide particles (AS). The three composites, in the form of short lengths of uncooled tubes, were exposed to 900°C flue gases in the waste incinerator for intermittent periods during the time (up to 6 months) the tubes were in the incinerator.

The alumina matrix of the continuous filament composites was penetrated by several flue gas constituents: Na, Si, P, and S. Sodium, K, and S were also identified at the midpoint of one of the composites, indicating penetration to a depth of at least 1.5 mm. These elements probably penetrated the alumina matrix through porosity, which was about 35% in this material. Compositional differences between the center and edge of filaments, especially near the surface of 166A, were detected; otherwise, no new compounds or other microstructural changes were observed. The zirconia coating originally applied to the outer surface of some composite tubes mostly spalled and did not survive the exposure; therefore, both 166A and 166A/Z behaved similarly in this test, and the ability of the coating to resist penetration of flue gas constituents was not assessed.

There was less penetration of flue gas constituents into 166Z, possibly because the matrix had a porosity of only about 25%. The extent of reaction at the surface, however, was significantly greater in 166Z than in 166A. Two distinct reaction layers containing crystals formed on the surface. Aluminum, Na, Si, S, and, possibly, Sb and Sn were present in the

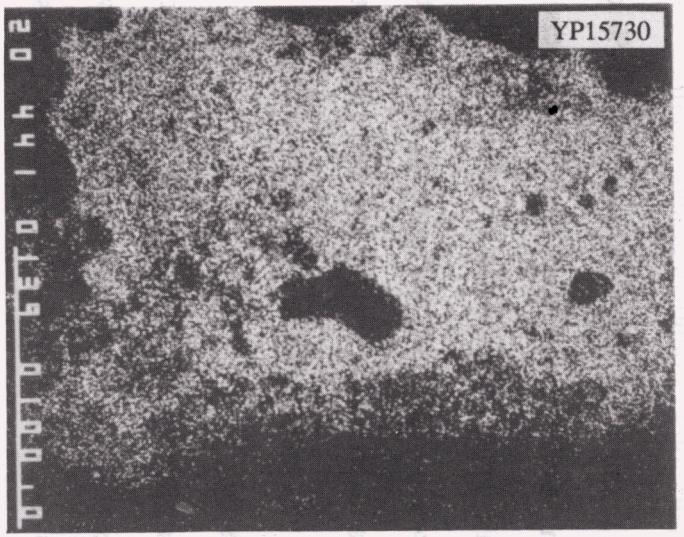

(*d*) Na

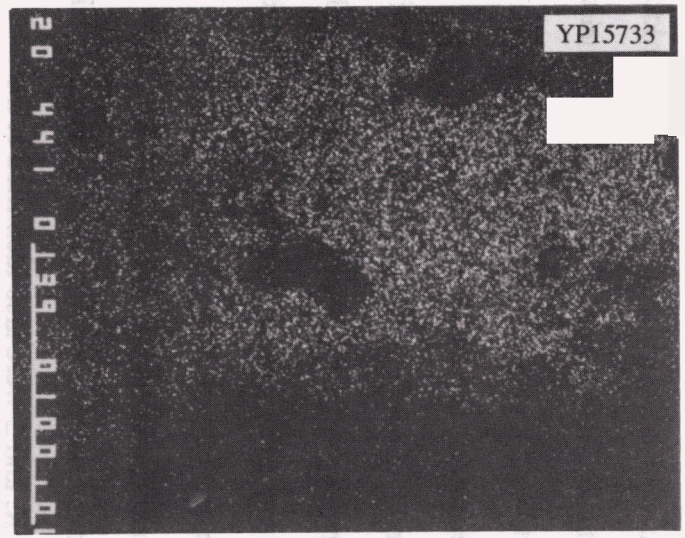

(*e*) S

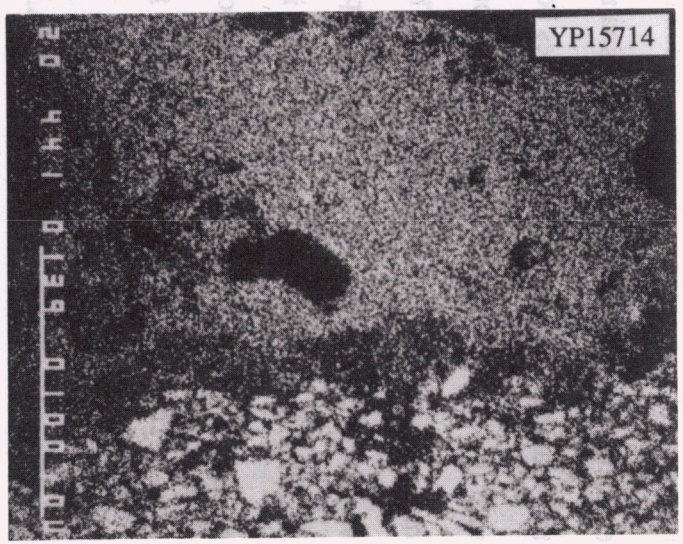

(*f*) Si

Fig. 22. (continued)

evidently resisted penetration of flue gas constituents because the alumina matrix was much denser than that of the continuous-filament composites.

The reason for higher susceptibility of 166Z to degradation has not been determined. Perhaps the lower porosity of the zirconia matrix, compared to the alumina matrix, effectively retains and concentrates more of the constituents on the surface, whereas the more porous alumina matrix allows dilution by penetration.

The following conclusions, derived from the results of microstructural examinations, pertain specifically to the 6-month exposure:

1. continuous-filament ceramic composites 166A and 166Z were penetrated by flue gas constituents, the former more than the latter;
2. even though 166A was penetrated with flue gas constituents, a significant amount of new compounds was not observed within the filaments or matrix, suggesting that their concentrations might have been too small to cause significant compound formation;
3. only a slight reaction layer occurred at the surface of 166A, but there were compositional changes in near-surface filaments as well as to filaments well below the surface;
4. a more extensive reaction layer occurred at the surface of 166Z, resulting in severe attack of filaments near the surface; and
5. a layer was evident on the surface of the AS composite, but there was no indication the silicon carbide particles near the interface were attacked.

In comparing the relatively porous continuous-filament composites 166A and 166Z, the latter, as evidenced by attack of the filaments in a reaction layer, is more susceptible to degradation by reaction with flue gas constituents even though gas penetration is less. On the other hand, the much denser AS composite, with its alumina matrix and aluminosilicate

surface coating, had a significant surface layer but no evidence of an extensive reaction. These results suggest that the alumina, whether in a porous or dense form, is resistant to the incinerator constituents at the concentrations present in these tests. It is to be noted that previous tests with higher concentrations of sodium showed reaction of the alumina with the sodium. If the exposure temperature substantially exceeded 900°C during an extended temperature excursion, or if the exposure times were substantially longer than 6 months, the amount of degradation might be substantially more than was found in the examinations described herein.

6. ACKNOWLEDGMENTS

The authors wish to acknowledge the contributions of other ORNL personnel to this report: J. R. Mayotte and C. P. Haltom for preparation of specimens for light microscope examination, photography, and electron microprobe analyses and photographs. We thank R. E. Pawel and A. E. Pasto for reviewing the draft and for helpful suggestions. Finally, we thank G. R. Carter for final preparation of the report and K. Spence for editing.

7. REFERENCES

1. A. J. Hayes and S. L. Richlen, "The Department of Energy's Advanced Heat Exchangers Program," pp. 21-27 in *Proceedings of the Conference on Industrial Heat Exchangers*, ed. A. J. Hayes, W. W. Liang, S. L. Richlen, and E. S. Tabb, Pittsburgh, November 6-8, 1985.

2. S. L. Richlen, "Research for Advanced Heat Exchangers—The U.S. DOE Program," pp. 31-36 in *Eighth Annual Industrial Energy Technology Conference & Exhibition*, Vol. 1, Houston, June 17-19, 1986.

3. J. E. Snyder and W. P. Parks, Jr., "Research and Development of a Ceramic Fiber Composite Heat Exchanger—Phase I," DOE contract DE-AC-07-84ID12536-1, Babcock & Wilcox Company, Lynchburg, Va., July 1985.

4. W. P. Parks, Jr., "Research and Development of a Ceramic Fiber Composite Heat Exchanger—Phase II," DOE contract DE-AC-07-84ID12536-2, Babcock & Wilcox Company, Lynchburg, Va., April 1990.

5. J. I. Federer, "Corrosion Behavior of Continuous-Filament-Wound Ceramic Composite Tubes," ORNL/TM-11691, Martin Marietta Energy Systems, Inc., Oak Ridge Natl. Lab., May 1991.

INTERNAL DISTRIBUTION

1-2. Central Research Library
3. Document Reference Section
4-5. Laboratory Records Department
6. Laboratory Records, ORNL RC
7. ORNL Patent Section
8-10. M&C Records Office
11. H. G. Arnold
12. R. L. Beatty
13. P. F. Becher
14. T. M. Besmann
15. R. S. Carlsmith
16. N. C. Cole
17. D. F. Craig
18. J. H. Devan
19-23. J. I. Federer
24. M. K. Ferber
25. F. M. Foust
26. E. L. Fuller, Jr.
27. M. L. Grossbeck
28-32. T. J. Henson
33. M. G. Jenkins
34. M. A. Karnitz
35-44. J. R. Keiser
45. A. S. Loebl
46. R. A. Lowden
47. J. R. Mayotte
48. A. E. Pasto
49. W. D. Porter
50. P. L. Rittenhouse
51. P. S. Sklad
52. G. M. Slaughter
53. D. P. Stinton
54. V. J. Tennery
55. P. F. Tortorelli
56. A. A. Wereszczak
57. D. F. Wilson
58. Y. A. Chang (Consultant)
59. H. W. Foglesong (Consultant)
60. J. J. Hren (Consultant)
61. M. L. Savitz (Consultant)
62. J. G. Simon (Consultant)
63. K. E. Spear (Consultant)

EXTERNAL DISTRIBUTION

64. AMERCOM, 8928 Fullbright Avenue, Chatsworth, CA 91311

    W. E. Beyermann

65. ARGONNE NATIONAL LABORATORY, 9700 South Cass Ave., Argonne, IL 60439

    K. Natesan

66-67. BABCOCK AND WILCOX, R&D Division, 1562 Beeson Street, Alliance, OH 44601

    C. L. DeBellis
    J. B. Sandifer

68-76. BABCOCK AND WILCOX, P.O. Box 11165, Lynchburg, VA 24505

    E. A. Barringer
    D. L. Baty
    R. W. Goettler
    D. L. Hindman (5)
    W. G. Long

77-78. CARBORUNDUM COMPANY, P.O. Box 337, 1625 Buffalo Ave., Niagara Falls, NY 14302

C. Ebel
R. Storm

79-80. CARBORUNDUM COMPANY, P.O. Box 1054, Niagara Falls, NY 14302

J. M. Bevilacqua
M. C. Kerr

81. CONSOLIDATED NATURAL GAS, 11001 Cedar Avenue, Cleveland, OH 44106

J. Bjerklie

82-83. COORS CERAMICS CO., 17750 West 32 Ave., Golden CO 80401

P. Dibillis
J. Sibold

84. DOW CORNING CORPORATION, 3901 South Saginaw Road, Midland, MI 48640

W. H. Atwell

85. DOW CORNING CORPORATION, Suite 325 South, 1800 M. Street, N.W., Washington, DC 20036

J. K. Wessel

86. DREXEL UNIVERSITY, Building 27-439, Philadelphia, PA 19104

F. Ko

87-88. GAS RESEARCH INSTITUTE, 8600 W. Bryn Mawr Ave., Chicago, IL 60631

S. Freedman
M. A. Lukasiewicz

89-90. GENERAL ELECTRIC COMPANY, GE Corporate Research and Development, P.O. Box 8, Schenectady, NY 12301

H. W. Lake, Bldg. KW, Rm. C258
F. N. Mazandarany, Bldg. K-1, MB-259

91. GENERAL MOTORS CORPORATION, Allison Gas Turbine Division, BF Goodrich, Aerospace, P.O. Box 420, Indianapolis, IN 46206-0420

C. Wilkes

92. HAGUE INTERNATIONAL , 3 Adams St., South Portland, ME 04106

W. Dunlay

93-95. LANXIDE CORPORATION, 1300 Marrows Road, P.O. Box 6077, Newark, DE 19714-6077

D. J. Landini
A. N. Patel (MS6077)
K. G. White (MS6104)

96. MASSACHUSETTS INSTITUTE OF TECHNOLOGY, 77 Mass. Ave., Rm. 12-009, Cambridge, MA 02139

J. S. Haggerty

97-98. NORTON COMPANY, 1 New Bond Street, Worcester, MA 01606

B. D. Foster
K. Green

99. PAR ENTERPRISE, INC., 12601 Clifton Hunt Lane, Clifton, VA 22024

W. J. Rebello

100. PENNSYLVANIA STATE UNIVERSITY, 227 Hammond Building, University Park, PA 16802

H. T. Hahn

101. PENNSYLVANIA STATE UNIVERSITY, 513A Deike Building, University Park, PA 16802

J. R. Hellmann

102. POWER GENERATION CONSULTANTS, 1261 Post House Lane, Media, PA 19063

M. DeCorso

103-104. REFRACTORY COMPOSITES, INC., 12220-A Rivera Rd., Whittier, CA 90606

K. Kratsch
E. L. Paquette

105-107. SOLAR TURBINES INCORPORATED, P.O. BOX 85376, San Diego, CA 92138-5376

B. Harkins
V. M. Parthasarathy
M. Van Roode

108. G. SORELL CONSULTING SERVICES MATERIALS/CORROSION ENGINEERING, 49 Brookside Terrace, North Caldwell, NJ 07006

J. Sorell

109-111. STONE & WEBSTER ENGINEERING CORPORATION, 245 Summer Street, Boston, MA 02107

L. J. McDonough
R. A. Rosenberg
J. J. Williams

112. SULLIVAN MINING CORPORATION, P.O.Box 4615, San Diego, CA 92121

T. M. Sullivan

113. TEXTRON, INC., 2 Industrial Ave., Lowell, MA 01851

B. N. Thompson

114. UNIVERSITY OF ILLINOIS AT CHICAGO, P.O. Box 4348, Chicago, IL 60680

M. J. McNallan

115. UNIVERSITY OF TENNESSEE SPACE INSTITUTE, MS 3, Tullahoma, TN 37388

W. H. Boss

116-117. U.S. DOE, CHICAGO FIELD OFFICE, 9800 S. Cass Avenue, Argonne, IL 60439

J. E. Jonkouski
J. Mavec

118-126. U.S. DOE, MORGANTOWN ENERGY TECHNOLOGY CENTER, P.O. Box 880, Morgantown, WV 26505

R. A. Bajura
R. C. Bedick
D. C. Cicero
F. W. Crouse, Jr.
N. T. Holcombe
W. J. Huber
M. J. Mayfield
J. E. Notestein
J. S. Wilson

127. U.S. DOE, OFFICE OF BASIC ENERGY SCIENCES, Materials Sciences Division, ER-131 GTN, Washington, DC 20545

J. B. Darby

128. U.S. DOE, OFFICE OF CONSERVATION AND RENEWABLE ENERGY, CE-12 Forrestal Building, Washington, DC 20545

J. J. Eberhardt

129. U.S. DOE, OFFICE OF FOSSIL ENERGY, Washington, DC 20545

J. P. Carr (FE-14) GTN

130-132. U.S. DOE, OFFICE OF INDUSTRIAL TECHNOLOGIES, 1000 Independence Avenue, Forrestal Building, Washington, DC 20585

J. Eustis
W. P. Parks, Jr.
S. L. Richlen

133-136. U.S. DOE, PITTSBURGH ENERGY TECHNOLOGY CENTER, P.O. Box 10940, Pittsburgh, PA 15236

A. H. Baldwin
G. V. McGurl
R. Santore
T. M. Torkos

137-138. U.S. DOE, OAK RIDGE FIELD OFFICE, Oak Ridge National Laboratory, P.O. Box 2008, Oak Ridge, TN 37831-6269

E. E. Hoffman
G. Riner

139-148. U.S. DOE, OFFICE OF SCIENTIFIC AND TECHNICAL INFORMATION, P.O. Box 62, Oak Ridge, TN 37831

For distribution by microfiche as shown in DOE/OSTI-4500, Distribution Category UC-310 [Industrial Programs (General)]